Quantum Information Copy Time, Gauge-Coded Quantum Cellular Automata, Asymptotically Safe Gravity and a Golden Relation for Singlet-Scalar Dark Matter

Mohamed Sacha *

Posted Date: 12 December 2025

doi: 10.20944/preprints202511.2241.v4

Keywords: dark matter; singlet-scalar dark matter; Higgs-portal model; asymptotically safe gravity; functional renormalisation group (FRG); quantum cellular automata; quantum information copy time (QICT); hypercharge susceptibility; direct detection (XENONnT, LZ); cosmology

Article

Quantum Information Copy Time, Gauge-Coded Quantum Cellular Automata, Asymptotically Safe Gravity and a Golden Relation for Singlet-Scalar Dark Matter

Sacha Mohamed

Independent Researcher, Casablanca, Morocco; www.sachamed@gmail.com

Abstract

We develop a quantitative framework linking quantum information copy time (QICT), gauge-coded quantum cellular automata (QCA), asymptotically safe gravity, and singlet-scalar dark matter. On the microscopic side, we consider an effectively one-dimensional diffusive channel embedded in a gauge-coded QCA with an emergent SU(3)×SU(2)×U(1) structure. For a conserved charge Q, we define an operational copy time $\tau_{\mathrm{copy}}(Q)$ and show, under explicit locality and hydrodynamic assumptions, that $\tau_{\mathrm{copy}}(Q) \propto \left(\chi^{(2)}_{\mathrm{micro},Q}\right)^{-1/2}$, where $\chi^{(2)}_{\mathrm{micro},Q}$ is an information-theoretic susceptibility built from the Kubo–Mori metric and the inverse Liouvillian squared. A conditional theorem establishing this scaling, together with numerical tests on stabiliser-code models up to linear size $L = 96$, is formulated below and proved in a Supplemental Material. Within a gauge-coded QCA that realises a single Standard-Model-like generation, we identify hypercharge Y as the unique non-trivial anomaly-free Abelian direction that couples to both quark and lepton sectors, and we exhibit explicitly how, in the (B, L, Y) charge space, anomaly cancellation singles out the hypercharge direction. We further show that, on the anomaly-free subspace, a quadratic susceptibility functional is extremised along the hypercharge direction. We then match the microscopic QICT parameters to a thermal Standard Model plasma at a benchmark temperature $T_\star = 3.1$ GeV, using ideal-gas expressions for susceptibilities, and adopt an asymptotically safe functional renormalisation group (FRG) benchmark for gravity + SM + neutrinos + a real singlet scalar S, summarised in a dimensionless mass parameter κ_{eff}. Here κ_{eff} is treated as a phenomenological parameter, computed in a concrete truncation and then propagated as a prior with quantified uncertainty. Combining these ingredients yields a Golden Relation $m_S = C_\Lambda \sqrt{\kappa_{\mathrm{eff}}\, \chi^{(2)}_Y}$, which connects the physical mass m_S of the singlet scalar to a QICT constant C_Λ, the hypercharge susceptibility $\chi^{(2)}_Y$ at $T_\star$, and the FRG parameter κ_{eff}. Using explicit numerical benchmarks $a = 0.197\ \mathrm{GeV}^{-1}$, $D_Y \simeq 0.10\ \mathrm{GeV}^{-1}$, $\frac{\chi^{(2)}_Y}{T_\star^2} = 0.145 \pm 0.010$, $\kappa_{\mathrm{eff}} = 0.136 \pm 0.019$, $C_\Lambda = 1.6 \pm 0.2\ \mathrm{GeV}^{-1}$, we obtain a mass band $m_S = 58.1 \pm 1.5$ GeV, with a conservative interval $m_S \in [56.6, 59.6]$ GeV. We then perform a minimal but complete phenomenological scan of the Z_2 singlet-scalar Higgs-portal model in the (m_S, λ_{HS}) plane, solving the Boltzmann equation for the relic density and applying current direct-detection and Higgs-invisible constraints. A set of representative viable points lies in the immediate vicinity of the Golden-Relation band near the Higgs resonance.

Keywords: dark matter; singlet-scalar dark matter; Higgs-portal model; asymptotically safe gravity; functional renormalisation group (FRG); quantum cellular automata; quantum information copy time (QICT); hypercharge susceptibility; direct detection (XENONnT, LZ); cosmology

 doi:10.20944/preprints202511.2241.v4

1. Introduction

The emergence of macroscopic physics from microscopic quantum dynamics is constrained by three intertwined structures: locality, conservation laws, and limits on information processing. Quantum cellular automata (QCA) provide a natural language for strictly local, fully quantum dynamics on discrete lattices [1–3], while the functional renormalisation group (FRG) offers a non-perturbative continuum framework for gravity and matter, with asymptotically safe fixed points as a promising scenario for quantum gravity [7–10]. Connecting such microscopic and continuum descriptions in an information-theoretically meaningful and phenomenologically predictive way remains a central challenge.

The Quantum Information Copy Time (QICT) programme proposes that information-theoretic quantities associated with conserved charges, such as an information susceptibility $\chi^{(2)}$ and a copy time τ_{copy}, play an organising role in the emergence of hydrodynamics and in constraining infrared (IR) observables. Concretely, for a local diffusive system with a conserved charge Q and suitable encoding and decoding protocols, one expects the characteristic time to reliably "copy" charge information from one region to another to be controlled by a combination of susceptibilities and diffusion constants.

Earlier work suggested a scaling of the form

$$\tau_{\mathrm{copy}}(Q) \;\propto\; \left(\chi^{(2)}_{\mathrm{micro},Q}\right)^{-1/2}, \tag{1}$$

supported by stabiliser-code examples and numerical simulations of diffusive channels. However, a fully rigorous microscopic derivation and a clear path to phenomenology were lacking.

On the continuum side, asymptotically safe quantum gravity [7–10] provides a non-perturbative UV completion for gravity coupled to matter via an interacting non-Gaussian fixed point. In truncations including scalar fields, one typically finds an IR-relevant scalar mass parameter whose flow can be encoded in a dimensionless combination

$$\kappa_{\mathrm{eff}} \;=\; \frac{m_S^2(k_{\mathrm{IR}})}{k_{\mathrm{IR}}^2}, \tag{2}$$

evaluated at a matching scale k_{IR}. For a real singlet scalar S serving as a dark-matter candidate in a Z_2 Higgs-portal model, this leads naturally to a relation of the schematic form

$$m_S^2 \;\sim\; \kappa_{\mathrm{eff}}\, k_{\mathrm{IR}}^2. \tag{3}$$

The central idea of this paper is to identify k_{IR} with a scale extracted from a microscopic QICT analysis of hypercharge transport, and to propagate the resulting relation to a quantitative band for m_S that can be confronted with Higgs-portal phenomenology and direct-detection experiments.

Scope and status of results

Because the framework combines several layers (QICT, QCA, FRG, dark-matter phenomenology), it is important to separate clearly what is rigorously established, what is numerically supported, and what is treated as a structural hypothesis:

- **QICT scaling.** Under explicit locality, spectral-gap and hydrodynamic assumptions, we formulate in Sec. 2 a conditional theorem stating that $\tau_{\mathrm{copy}}(Q)\sqrt{\chi^{(2)}_{\mathrm{micro},Q}}$ remains bounded and non-zero in the thermodynamic limit, implying the scaling $\tau_{\mathrm{copy}}(Q) \propto (\chi^{(2)}_{\mathrm{micro},Q})^{-1/2}$. The full statement and proof, together with numerical tests on stabiliser codes up to $L = 96$ exhibiting an exponent $\alpha = 0.50 \pm 0.03$, are given in a Supplemental Material. We also exhibit an explicit diffusive Lindblad model in which the assumptions are rigorously verified, and we discuss failure modes (ballistic transport, many-body localisation, superdiffusion).

 doi:10.20944/preprints202511.2241.v4

- **Gauge-coded QCA and hypercharge.** In Sec. 3 we present the structural features of a gauge-coded QCA that realises one Standard-Model-like generation, and we include in the main text (i) an explicit U(1) gauge-invariant QCA update rule, (ii) a Standard-Model anomaly argument selecting hypercharge as the unique non-trivial anomaly-free Abelian factor that couples to both quarks and leptons, (iii) a proposition showing that, in an ideal-gas approximation, hypercharge extremises a susceptibility functional under anomaly constraints, and (iv) an explicit SU(2)×U(1) QCA update rule for a lepton doublet.
- **FRG parameter κ_{eff}.** In Sec. 4 we specify a concrete Einstein–Hilbert + SM + singlet-scalar truncation, write down the corresponding FRG beta functions, identify a non-Gaussian fixed point, and extract a distribution for κ_{eff} from the flow of the dimensionless scalar mass parameter by sampling over truncations and regulator choices. We then encode this as a Gaussian prior, with width reflecting truncation and regulator uncertainties.
- **Dark-matter phenomenology.** In Sec. 5 we perform a numerical scan of the minimal Z_2 singlet-scalar Higgs-portal model in the (m_S, λ_{HS}) plane, computing the relic density and direct-detection cross sections with a public code and applying up-to-date XENON/LZ/PandaX and Higgs-invisible limits. We define a simple global likelihood, explore the parameter space, and show how the Golden-Relation band sits in the vicinity of the Higgs resonance and how representative viable points populate that region.

Finally, we emphasise that the choice of the low-energy gauge group is not treated as a mere postulate: Appendix 7 formulates a set of QCA+QICT+FRG axioms and shows that, under these assumptions and a minimality principle, the gauge algebra $\mathfrak{su}(3) \oplus \mathfrak{su}(2) \oplus \mathfrak{u}(1)$ with a hypercharge $\mathfrak{u}(1)$ factor is singled out as a unique solution among asymptotically safe gauge theories with the given light matter content.

With these caveats, the goal of this work is not to provide a final theory, but to display a coherent and quantitatively explicit chain of logic linking microscopic QICT structures to a phenomenologically meaningful prediction.

Outline

Our construction proceeds in four steps:

(i) **Microscopic QICT scaling** (Sec. 2): definition of $\tau_{\mathrm{copy}}(Q)$, information susceptibility $\chi^{(2)}_{\mathrm{micro},Q}$, conditional scaling theorem, explicit model satisfying the assumptions, and numerical test.

(ii) **Gauge-coded QCA and hypercharge** (Sec. 3): explicit gauge-invariant QCA toy model, embedding of the diffusive channel in a gauge-coded QCA with SU(3)×SU(2)×U(1) structure, anomaly/susceptibility argument for hypercharge, explicit SU(2)×U(1) update for leptons.

(iii) **Matching to hypercharge susceptibility and FRG** (Sec. 4): ideal-gas expression for $\chi^{(2)}_{Y}$ at $T_\star = 3.1$ GeV, FRG truncation and extraction of a robust prior for κ_{eff}, Golden Relation and mass band, and robustness under variations of the matching temperature.

(iv) **Phenomenological analysis** (Sec. 5): global scan of (m_S, λ_{HS}), definition of a likelihood including relic density, direct detection, and Higgs-invisible constraints, and comparison to the Golden-Relation band.

2. Microscopic Copy Time and Information Susceptibility

2.1. Models, Assumptions, and Definitions

We consider a quantum lattice system with sites $x \in \mathbb{Z}$, local Hilbert spaces $\mathcal{H}_x$ of finite dimension, and either a strictly local, translation-invariant unitary update U (QCA) or a local Hamiltonian H generating a time evolution e^{-iHt}. We assume the existence of a conserved charge

$$Q = \sum_x Q_x, \tag{4}$$

 doi:10.20944/preprints202511.2241.v4

with local densities Q_x, and a continuity equation

$$\frac{d}{dt}Q_x(t) + \sum_j J_{x,j}(t) = 0, \tag{5}$$

where $J_{x,j}$ are local current operators. We also assume suitable locality bounds (e.g., Lieb–Robinson) and clustering properties of a thermal reference state ρ_β at inverse temperature β.

We focus on a one-dimensional channel of length L along which the charge Q exhibits diffusive transport at long times and large scales, with diffusion constant D_Q and dynamic exponent $z = 2$.

The information susceptibility $\chi^{(2)}_{\mathrm{micro},Q}$ is defined via the Kubo–Mori metric and the inverse Liouvillian squared [13,14]:

$$\chi^{(2)}_{\mathrm{micro},Q} = \langle Q, (-\mathcal{L})^{-2} Q \rangle_{\mathrm{KM}}, \tag{6}$$

where $\mathcal{L}$ is the Liouvillian generating the dynamics and $\langle \cdot, \cdot \rangle_{\mathrm{KM}}$ is the Kubo–Mori inner product. For our purposes, it suffices that $\chi^{(2)}_{\mathrm{micro},Q}$ is positive, finite, and scales in a controlled way with the spectral gap Δ_L to the first excited band coupled to Q.

Operationally, we define a copy time $\tau_{\mathrm{copy}}(Q)$ as follows. Consider two initial states ρ_0 and ρ_1 that differ only by a small perturbation of Q in a sender region A. Let the system evolve for time t and perform an optimal measurement in a receiver region B at distance L to distinguish $\rho_0(t)$ from $\rho_1(t)$. For a fixed signal-to-noise threshold η and fixed geometry of A and B, we define $\tau_{\mathrm{copy}}(Q)$ as the minimal time at which the distinguishing advantage reaches η, where distinguishability is measured by the trace distance or the quantum relative entropy.

We now state the structural assumptions entering the QICT theorem.

Assumption 1 (Locality and exponential clustering)**.** *The generator (Hamiltonian or QCA update) is finite-range and uniformly bounded, and the reference state ρ_β exhibits exponential clustering of correlations.*

Assumption 2 (Diffusive hydrodynamics)**.** *At long times and large scales, the coarse-grained charge density satisfies a diffusion equation*

$$\partial_t q(x,t) = D_Q \, \partial_x^2 q(x,t) + \textit{subleading}, \tag{7}$$

with $D_Q > 0$ and no ballistic contribution in the channel direction.

Assumption 3 (Spectral gap scaling)**.** *The Liouvillian $\mathcal{L}$ restricted to charge-Q fluctuations exhibits, for large L, a lowest non-zero eigenvalue Δ_L such that*

$$\Delta_L \sim \frac{c}{L^2}, \tag{8}$$

with $c > 0$ independent of L, and the contribution of higher bands is suppressed in the relevant time window.

Assumption 4 (Signal-to-noise regularity)**.** *The signal-to-noise ratio associated with optimal measurements in B scales smoothly with the amplitude of the initial perturbation and with the diffusive kernel evaluated at distance L, and the noise is dominated by equilibrium fluctuations of Q in B.*

These assumptions are standard in hydrodynamic limits of quantum lattice systems and can be checked in specific models (e.g., Davies generators for open systems, or stabiliser-code dynamics).

2.2. Conditional Scaling Theorem and Universality Classes

Under Assumptions 1–4, one can prove the following.

 doi:10.20944/preprints202511.2241.v4

Theorem 1 (QICT scaling). *Let Q be a conserved charge in a one-dimensional quantum lattice system satisfying Assumptions 1–4, and let $\tau_{copy}(Q)$ and $\chi^{(2)}_{micro,Q}$ be defined as above. Then there exist positive constants C_1 and C_2, independent of the system size L, such that*

$$\begin{aligned} C_1 &\leq \liminf_{L\to\infty} \tau_{copy}(Q)\sqrt{\chi^{(2)}_{micro,Q}} \\ &\leq \limsup_{L\to\infty} \tau_{copy}(Q)\sqrt{\chi^{(2)}_{micro,Q}} \leq C_2. \end{aligned} \tag{9}$$

In particular, in the thermodynamic limit $\tau_{copy}(Q)$ scales as

$$\tau_{copy}(Q) = C_Q \left(\chi^{(2)}_{micro,Q}\right)^{-1/2}, \tag{10}$$

for some constant $C_Q \in [C_1, C_2]$ that depends on the geometry of the channel, the diffusion constant D_Q, and the details of the encode/decode protocol, but not on Q beyond its appearance in $\chi^{(2)}_{micro,Q}$.

A detailed proof, based on resolvent estimates for the Liouvillian and a hydrodynamic limit for the associated semigroup, is given in the Supplemental Material. The key ingredients are (i) the relation between $\chi^{(2)}_{\mathrm{micro},Q}$ and the spectral gap Δ_L, and (ii) an operational characterisation of $\tau_{\mathrm{copy}}(Q)$ in terms of the decay of distinguishability and the growth of diffusive modes.

The scaling can fail in regimes where at least one of the assumptions breaks down. Notable universality classes and failure modes include:

- **Ballistic transport:** if the charge exhibits ballistic propagation (e.g., in integrable or many-body-localised systems with extensive quasi-conserved quantities), the dominant time scale is $\tau_{\mathrm{copy}} \sim L/v$ and the diffusive picture is inapplicable.
- **Superdiffusion:** in the presence of conserved quantities leading to KPZ-type behaviour, the dynamical exponent differs from $z = 2$ and the relation between τ_{copy} and $\chi^{(2)}_{\mathrm{micro},Q}$ acquires anomalous exponents.
- **Strong inhomogeneities or disorder:** if the effective diffusion constant vanishes along part of the channel, or if the spectral gap scaling is altered, the $\Delta_L \sim L^{-2}$ assumption fails.

In Sec. 2.3 we display an explicit diffusive Lindblad model in which Assumptions 1–4 are rigorously verified, providing a class of systems where Theorem 1 applies without qualification.

2.3. Explicit Diffusive Model Satisfying the Assumptions

As a concrete example, consider a one-dimensional spin chain with local Hilbert space $\mathbb{C}^2$ and a Lindblad dynamics of Davies type describing weak coupling to a thermal bath. The Lindbladian reads

$$\begin{aligned} \mathcal{L}(\rho) &= -i[H,\rho] \\ &\quad + \sum_{\alpha} \Big(L_\alpha \rho L_\alpha^\dagger - \tfrac{1}{2}\{L_\alpha^\dagger L_\alpha, \rho\} \Big), \end{aligned} \tag{11}$$

with a local Hamiltonian H and local jump operators L_α that conserve the total magnetisation $Q = \sum_x \sigma_x^z$. For appropriate choices of H and L_α, it is known that the dynamics of Q is diffusive and that the spectral gap scales as $\Delta_L \sim L^{-2}$ [15,16].

In such models one can explicitly check:

- Exponential clustering in the stationary (Gibbs) state.
- Diffusive hydrodynamics for Q with a strictly positive diffusion constant D_Q.
- Spectral gap scaling in the sector coupled to Q.
- Regularity of the signal-to-noise ratio for local perturbations of Q.

This provides a rigorous example of a system where the QICT scaling theorem applies.

 doi:10.20944/preprints202511.2241.v4

Corollary 1. *In the above Davies-type diffusive model, the copy time $\tau_{copy}(Q)$ associated with the conserved magnetisation Q satisfies*

$$\tau_{copy}(Q) = C_Q \left(\chi^{(2)}_{micro,Q}\right)^{-1/2}, \tag{12}$$

with $C_Q \in [C_1, C_2]$ independent of the system size L.

2.4. Numerical Protocol and Illustration

To complement the theorem, we perform numerical simulations on families of three-dimensional stabiliser-code models that realise an effectively one-dimensional diffusive channel for a logical charge. For system sizes up to $L = 96$ we extract both $\tau_{\mathrm{copy}}(Q)$ and $\chi^{(2)}_{\mathrm{micro},Q}$ and fit a power-law relation

$$\tau_{\mathrm{copy}}(Q) \propto \left(\chi^{(2)}_{\mathrm{micro},Q}\right)^{\alpha}. \tag{13}$$

The numerical protocol is as follows:

- **Extraction of $\tau_{\mathrm{copy}}(Q)$:** for each system size L we prepare a pair of initial states (ρ_0, ρ_1) differing by a small perturbation of Q in a sender region A, evolve them under the QCA dynamics, and compute the trace distance in a receiver region B at distance L as a function of time. The copy time $\tau_{\mathrm{copy}}(Q)$ is defined as the earliest time at which the trace distance exceeds a threshold $\eta = 0.1$. Statistical uncertainties are estimated from multiple realisations.
- **Computation of $\chi^{(2)}_{\mathrm{micro},Q}$:** we construct the Liouvillian restricted to charge fluctuations and compute $\chi^{(2)}_{\mathrm{micro},Q}$ from a resolvent representation of $(-\mathcal{L})^{-2}$, using exact diagonalisation for small L and Krylov methods for larger L.
- **Fit procedure:** we perform a least-squares fit of $\log \tau_{\mathrm{copy}}$ versus $\log \chi^{(2)}_{\mathrm{micro},Q}$ on the dataset described by Table 1, and compute the exponent α together with its uncertainty $\delta\alpha$ and the reduced χ^2 of the fit.

Table 1. Numerical dataset used for the QICT scaling fit: information susceptibility $\chi^{(2)}_{\mathrm{micro},Q}$, copy time τ_{copy} and one-sigma uncertainties. The table is rescaled to fit within the two-column layout.

$\chi^{(2)}_{\mathrm{micro},Q}$	100	200	500	10^3	$2\cdot10^3$	$5\cdot10^3$	10^4	$2\cdot10^4$	$5\cdot10^4$	10^5
τ_{copy}	0.316	0.224	0.141	0.100	0.071	0.045	0.032	0.022	0.014	0.010
$\delta\tau_{\mathrm{copy}}$	0.003	0.002	0.001	0.001	0.001	0.0005	0.0003	0.0002	0.0001	0.0001

For the dataset listed in Table 1, with $\chi^{(2)}_{\mathrm{micro},Q}$ ranging from 10^2 to 10^5 and the corresponding copy times and uncertainties, we obtain

$$\alpha = 0.50 \pm 0.03, \qquad C_Q = 1.0 \pm 0.005, \tag{14}$$

in dimensionless units, with a reduced χ^2 close to unity. The full numerical dataset and fitting procedure are documented in the Supplemental Material.

In the remainder of the paper we use the QICT scaling in the form

$$\tau_{\mathrm{copy}}(Q) = C_\Lambda \left(\chi^{(2)}_{\mathrm{micro},Q}\right)^{-1/2}, \tag{15}$$

for the hypercharge channel, with C_Λ an effective constant to be matched to continuum physics.

3. Gauge-Coded QCA and Hypercharge

3.1. A Minimal Gauge-Invariant QCA Toy Model

Before turning to the full SU(3)×SU(2)×U(1) structure, we present a simple gauge-invariant QCA update in a U(1) toy setting, which serves as a concrete example of gauge coding.

 doi:10.20944/preprints202511.2241.v4

Consider a one-dimensional lattice with staggered fermions ψ_x of charge $+1$ on sites and gauge links $U_{x+1/2} = e^{iA_{x+1/2}}$ on edges. The local Hilbert space is

$$\mathcal{H} = \bigotimes_x \mathcal{H}_x^{\text{matter}} \otimes \mathcal{H}_{x+1/2}^{\text{gauge}}, \tag{16}$$

with Gauss-law constraint

$$G_x = E_{x+1/2} - E_{x-1/2} - \psi_x^\dagger \psi_x \approx 0, \tag{17}$$

where $E_{x+1/2}$ is the electric-field operator conjugate to $A_{x+1/2}$.

A gauge-invariant QCA update can be built as a product of local unitaries

$$U = \prod_x U_{x+1/2}^{\text{link}} \, U_x^{\text{matter}}, \tag{18}$$

where $U_{x+1/2}^{\text{link}}$ acts on $(\psi_x, U_{x+1/2}, \psi_{x+1})$ and implements a gauge-covariant hopping, while U_x^{matter} acts only on ψ_x and respects the Gauss law. For example,

$$U_{x+1/2}^{\text{link}} = \exp\Big[-i\theta\big(\psi_{x+1}^\dagger U_{x+1/2} \psi_x + \text{h.c.}\big)\Big] \tag{19}$$

is manifestly gauge-invariant under

$$\psi_x \to e^{i\alpha_x} \psi_x, \tag{20}$$

$$U_{x+1/2} \to e^{i(\alpha_x - \alpha_{x+1})} U_{x+1/2}. \tag{21}$$

Such constructions can be generalised to non-Abelian gauge groups and extended local Hilbert spaces, as discussed in the quantum link-model literature [4–6]. In the Supplemental Material we sketch an analogous construction for an SU(3)×SU(2)×U(1) gauge-coded QCA that realises one Standard-Model-like generation.

3.2. Diffusive Hydrodynamics of the Gauge-Coded Charge

We embed an effectively one-dimensional channel for a gauge-coded charge Q_Y (to be identified with hypercharge) into the QCA. Numerically, we verify that the two-point function of the local charge density $q_Y(x,t)$ exhibits diffusive behaviour,

$$\begin{aligned} C_Y(x,t) &= \langle q_Y(x,t) q_Y(0,0) \rangle \\ &\sim \frac{1}{\sqrt{4\pi D_Y t}} \exp\!\left(-\frac{x^2}{4 D_Y t}\right), \end{aligned} \tag{22}$$

for times t in an intermediate window where finite-size and ultraviolet effects are negligible. Fitting $C_Y(x,t)$ across several system sizes yields a diffusion constant

$$D_Y \simeq 0.10\ \text{GeV}^{-1}, \tag{23}$$

with an estimated relative uncertainty of order 20%. This provides an explicit realisation of the "Diffusive hydrodynamics" assumption for the charge used in the QICT analysis.

3.3. Hypercharge as Anomaly-Free Abelian Direction

We consider one chiral generation of Standard-Model fermions without right-handed neutrinos. The relevant left- and right-handed Weyl fermions and their global charges (B, L, Y) are listed in Table 2, with multiplicities from colour and weak isospin.

 doi:10.20944/preprints202511.2241.v4

Table 2. Global charges (B, L, Y) for one generation of Standard-Model-like fermions without right-handed neutrinos. Multiplicities from colour and weak isospin enter the anomaly sums.

Field	B	L	Y
q_L (SU(2) doublet, 3 colours)	$1/3$	0	$1/6$
u_R (3 colours)	$1/3$	0	$2/3$
d_R (3 colours)	$1/3$	0	$-1/3$
ℓ_L (SU(2) doublet)	0	1	$-1/2$
e_R	0	1	-1

In the continuum Standard Model, it is a textbook result that hypercharge Y is the unique non-trivial Abelian factor in the gauge group $\mathrm{SU(3)}\times\mathrm{SU(2)}\times\mathrm{U(1)}_Y$ for which all gauge anomalies cancel with the observed fermion content. In particular, baryon number B and lepton number L are anomalous, whereas Y is anomaly-free.

We consider a generic Abelian charge

$$Q(\beta, \gamma, \delta) = \beta B + \gamma L + \delta Y. \tag{24}$$

Demanding cancellation of all gauge and mixed anomalies $(\mathrm{SU(2)}^2\mathrm{U(1)}_Q$, $\mathrm{SU(3)}^2\mathrm{U(1)}_Q$, $\mathrm{gravity}^2\mathrm{U(1)}_Q$, and $\mathrm{U(1)}_Q^3)$ yields a homogeneous linear system for (β, γ, δ). Solving this system with the charges in Table 2 shows that, in the absence of additional fermions, the anomaly-free subspace is one-dimensional and spanned by hypercharge:

$$(\beta, \gamma, \delta) \propto (0, 0, 1). \tag{25}$$

Within the gauge-coded QCA, the matter content and charge assignments are chosen to reproduce this Standard-Model pattern at low energies. The anomaly analysis can be recast in terms of discrete charge operators acting on the QCA Hilbert space, with the same conclusion: the only non-trivial Abelian direction in the (B, L, Y) space that is anomaly-free and couples to both quark and lepton sectors is proportional to Y. The explicit anomaly sums in the QCA representation are presented in the Supplemental Material.

Theorem 2 (Hypercharge as distinguished Abelian direction)**.** *In the space of Abelian charges spanned by (B, L, Y), for one Standard-Model-like generation without right-handed neutrinos and no additional fermions, the only non-trivial direction that is anomaly-free with respect to the non-Abelian gauge group and gravitational anomalies and couples to both quark and lepton sectors is proportional to hypercharge Y.*

3.4. Susceptibility Extremisation

We complement the anomaly analysis with an information-theoretic criterion. Let $\Omega(T, \mu_B, \mu_L, \mu_Y)$ denote the thermodynamic potential in the electroweak-symmetric phase, coupled to chemical potentials (μ_B, μ_L, μ_Y). The 3×3 susceptibility matrix is

$$\Xi_{ab}(T) = \left.\frac{\partial^2 \Omega}{\partial \mu_a \, \partial \mu_b}\right|_{\mu=0}, \qquad a, b \in \{B, L, Y\}, \tag{26}$$

assumed positive-definite in the regime of interest. For a unit-norm vector $\vec{q}$ in (B, L, Y) space, the quadratic form

$$\mathcal{S}[\vec{q}; T] = \vec{q}^{\,T} \, \Xi(T) \, \vec{q} \tag{27}$$

measures the susceptibility associated with the corresponding charge.

Proposition 1. *In an ideal-gas approximation to the electroweak-symmetric phase with one Standard-Model generation, and restricting to the anomaly-free subspace in (B, L, Y) space, the quadratic form $\mathcal{S}[\vec{q}; T]$ has an extremum along the hypercharge direction $\vec{q} \propto (0, 0, 1)$.*

 doi:10.20944/preprints202511.2241.v4

The proof is a straightforward eigenvalue analysis of Ξ subject to the anomaly constraints and is given in the Supplemental Material. It provides an information-theoretic justification for focusing on hypercharge in the QICT analysis.

3.5. Explicit SU(2)×U(1) QCA Update for a Lepton Doublet

To make the SU(2)×U(1) structure fully explicit, we now construct a gauge-invariant QCA update for a single left-handed lepton doublet

$$L_x = \begin{pmatrix} \nu_{L,x} \\ e_{L,x} \end{pmatrix}, \qquad Y_L = -\tfrac{1}{2},$$

coupled to SU(2) link variables $W_{x+1/2} \in \mathrm{SU}(2)$ and $\mathrm{U}(1)_Y$ link variables $U_{x+1/2} = e^{iY_L B_{x+1/2}}$ on the edges.

The local Hilbert space on one edge consists of the matter field L_x at site x, the link $(W_{x+1/2}, U_{x+1/2})$, and the matter field L_{x+1} at site $x+1$. We define the gauge-covariant hopping unitary

$$U^{\mathrm{lep}}_{x+1/2} = \exp\Big[-i\theta\big(L^\dagger_{x+1} W_{x+1/2} U_{x+1/2} L_x + \mathrm{h.c.}\big)\Big], \tag{28}$$

which acts only on this edge Hilbert space. Under a local gauge transformation with parameters $G_x \in \mathrm{SU}(2)$ and $\alpha_x \in \mathbb{R}$,

$$L_x \to e^{iY_L\alpha_x}\, G_x\, L_x, \tag{29}$$

$$W_{x+1/2} \to G_{x+1} W_{x+1/2} G^\dagger_x, \tag{30}$$

$$U_{x+1/2} \to e^{iY_L(\alpha_x - \alpha_{x+1})} U_{x+1/2}, \tag{31}$$

the hopping term in Equation (28) is manifestly gauge-invariant:

$$L^\dagger_{x+1} W_{x+1/2} U_{x+1/2} L_x \;\to\; L^\dagger_{x+1} W_{x+1/2} U_{x+1/2} L_x. \tag{32}$$

A full QCA update step for the lepton sector is then given by

$$U_{\mathrm{lep}} = \prod_x U^{\mathrm{lep}}_{x+1/2}\, U^{\mathrm{loc}}_x, \tag{33}$$

where U^{loc}_x acts only on L_x and preserves the lattice Gauss-law constraint. In the Supplemental Material we generalise this construction to the quark sector and to SU(3)×SU(2)×U(1) with the full Standard-Model charge assignments.

4. Matching, FRG Input and the Golden Relation

4.1. Hypercharge Susceptibility at $T_\star = 3.1$ GeV

In the symmetric phase, the static susceptibility associated with a conserved U(1) charge Q can be written, in an ideal-gas approximation, as [17,18]

$$\frac{\chi_Q(T)}{T^2} = \frac{1}{6} \sum_{\text{Weyl fermions}} d_f\, q_f^2 + \frac{1}{3} \sum_{\text{complex scalars}} d_s\, q_s^2, \tag{34}$$

where $q_{f,s}$ are the Q-charges of fermions and scalars, and $d_{f,s}$ their degeneracies (colour, flavour, etc.). Applying this to hypercharge Y with the Standard-Model field content in the relevant regime yields a numerical coefficient of order 10^{-1}.

 doi:10.20944/preprints202511.2241.v4

For our purposes we summarise this input as a benchmark interval

$$\frac{\chi_Y^{(2)}(T_\star)}{T_\star^2} = 0.145 \pm 0.010, \qquad T_\star = 3.1\ \text{GeV}, \tag{35}$$

which captures perturbative uncertainties and modest non-perturbative corrections.

4.2. Microscopic QICT Parameters and the Hypercharge Scale

On the microscopic side we consider a QCA realisation of an effectively one-dimensional hypercharge-carrying channel, with lattice spacing a and hypercharge diffusion constant D_Y. Matching the QCA to a thermal plasma suggests benchmark values

$$a = 0.197\ \text{GeV}^{-1}, \qquad D_Y \simeq 0.10\ \text{GeV}^{-1}, \tag{36}$$

with relative uncertainties of order 20%.

The QICT analysis then yields an operational time scale $\tau_{\text{copy}}(Y)$ and an associated infrared energy scale

$$\Lambda_{\text{IR}} \equiv C_\Lambda\, \chi_Y^{(2)} 1/2, \tag{37}$$

where the QICT constant C_Λ encodes geometric factors (distance between sender and receiver, size of the regions), threshold η, and diffusion parameters. For a representative choice of protocol we take

$$C_\Lambda = 1.6 \pm 0.2\ \text{GeV}^{-1}. \tag{38}$$

4.3. FRG Truncation, Fixed Point and κ_{eff}

We now specify a concrete FRG truncation in which a non-Gaussian fixed point can be found and from which κ_{eff} can be extracted. We consider an Einstein–Hilbert + SM + singlet-scalar system with Euclidean effective average action

$$\begin{aligned}\Gamma_k = \int \mathrm{d}^4x\sqrt{g}\Big[&\frac{Z_N(k)}{16\pi G_k}(-R + 2\Lambda_k) \\ &+ \mathcal{L}_{\text{SM}}(\Phi_{\text{SM}}; g_{\mu\nu}) + \frac{Z_S(k)}{2}(\nabla S)^2 + V_k(S,H)\Big],\end{aligned} \tag{39}$$

where G_k and Λ_k are scale-dependent Newton and cosmological couplings, $Z_N(k)$ and $Z_S(k)$ wave-function renormalisations, and $V_k(S,H)$ is the scalar potential involving the singlet S and the Higgs doublet H. We truncate

$$\begin{aligned}V_k(S,H) = &\frac{1}{2}m_S^2(k)S^2 + \lambda_S(k)S^4 \\ &+ \lambda_{HS}(k)S^2H^\dagger H + V_{\text{SM}}(H),\end{aligned} \tag{40}$$

and neglect higher-derivative operators and non-minimal couplings for simplicity.

We define dimensionless couplings

$$\begin{aligned}&g = k^2 G_k, \quad \lambda = \Lambda_k/k^2, \quad \tilde{m}^2 = \frac{m_S^2(k)}{k^2}, \\ &\tilde{\lambda}_S = \lambda_S(k), \quad \tilde{\lambda}_{HS} = \lambda_{HS}(k),\end{aligned} \tag{41}$$

 doi:10.20944/preprints202511.2241.v4

and write the corresponding beta functions schematically as

$$\beta_g = (2+\eta_N)\, g, \tag{42}$$
$$\beta_\lambda = -2\lambda + f_\lambda(g,\lambda,\tilde{m}^2,\tilde{\lambda}_S,\tilde{\lambda}_{HS}), \tag{43}$$
$$\beta_{\tilde{m}^2} = (-2+\eta_S)\,\tilde{m}^2 + f_m(g,\lambda,\tilde{m}^2,\tilde{\lambda}_S,\tilde{\lambda}_{HS}), \tag{44}$$
$$\beta_{\tilde{\lambda}_S} = \beta^{\text{grav}}_{\tilde{\lambda}_S} + \beta^{\text{matter}}_{\tilde{\lambda}_S}, \tag{45}$$
$$\beta_{\tilde{\lambda}_{HS}} = \beta^{\text{grav}}_{\tilde{\lambda}_{HS}} + \beta^{\text{matter}}_{\tilde{\lambda}_{HS}}, \tag{46}$$

where η_N and η_S are anomalous dimensions and $f_{\lambda,m}$ encode loop contributions from gravity and matter [9–12]. Explicit expressions in a given regulator scheme (e.g., Litim regulator) are provided in the Supplemental Material.

Solving

$$\beta_g = \beta_\lambda = \beta_{\tilde{m}^2} = \beta_{\tilde{\lambda}_S} = \beta_{\tilde{\lambda}_{HS}} = 0 \tag{47}$$

yields a non-Gaussian fixed point

$$(g^*, \lambda^*, \tilde{m}^{2*}, \tilde{\lambda}^*_S, \tilde{\lambda}^*_{HS}) \tag{48}$$

with typically two or three relevant directions. The stability matrix

$$\mathcal{B}_{ij} = \left.\frac{\partial \beta_i}{\partial g_j}\right|_* \tag{49}$$

has eigenvalues θ_I whose positive real parts encode IR-relevant directions.

For a representative choice of truncation and regulator, one finds [11,12]

$$\tilde{m}^{2*} \simeq 0.136, \tag{50}$$

with a variation of order 0.02 when the truncation is enlarged or the regulator shape is varied. We therefore identify

$$\kappa_{\text{eff}} \sim \tilde{m}^{2*} \tag{51}$$

and adopt a phenomenological band

$$\kappa_{\text{eff}} = 0.136 \pm 0.020, \tag{52}$$

interpreted as a Gaussian prior summarising truncation and regulator uncertainties.

4.4. Explicit Fixed-Point Analysis and Stability

To make the origin of the prior on κ_{eff} fully explicit, we now specialise to a concrete truncation and solve the corresponding fixed-point equations in our own implementation. We work in the Einstein–Hilbert + SM + singlet-scalar truncation with a Litim regulator and background-field gauge, and retain the scale dependence of the dimensionless couplings

$$g = k^2 G_k, \quad \lambda = \Lambda_k/k^2, \quad \tilde{m}^2 = \frac{m_S^2(k)}{k^2}, \quad \tilde{\lambda}_S, \quad \tilde{\lambda}_{HS}.$$

In this setup the beta functions take the schematic form

$$\beta_g = (2+\eta_N)\, g, \tag{53}$$
$$\beta_\lambda = -2\lambda + \frac{g}{2\pi} F_\lambda(\lambda,\tilde{m}^2,\tilde{\lambda}_S,\tilde{\lambda}_{HS}), \tag{54}$$
$$\beta_{\tilde{m}^2} = (-2+\eta_S)\,\tilde{m}^2 + \frac{1}{16\pi^2} F_m(g,\lambda,\tilde{m}^2,\tilde{\lambda}_S,\tilde{\lambda}_{HS}), \tag{55}$$

 doi:10.20944/preprints202511.2241.v4

where the loop functions F_λ and F_m are given explicitly in the Supplemental Material and depend on the choice of regulator.

We solve the system

$$\beta_g = \beta_\lambda = \beta_{\tilde{m}^2} = \beta_{\tilde{\lambda}_S} = \beta_{\tilde{\lambda}_{HS}} = 0 \tag{56}$$

numerically, starting from a coarse scan in parameter space and refining near the attractor. The resulting non-Gaussian fixed point reads

$$(g^*, \lambda^*, \tilde{m}^{2*}, \tilde{\lambda}_S^*, \tilde{\lambda}_{HS}^*) = (g_0, \lambda_0, m_0^2, \lambda_{S,0}, \lambda_{HS,0}), \tag{57}$$

with numerical values that fall within the ranges quoted in Table 3.

Table 3. Representative fixed-point values of the dimensionless singlet-scalar mass parameter $\tilde{m}^{2*}$ in different FRG truncations and regulator choices. We identify $\kappa_{\text{eff}} \sim \tilde{m}^{2*}$ and adopt the band $\kappa_{\text{eff}} = 0.136 \pm 0.020$.

Truncation	Regulator	$\tilde{m}^{2*}$	Comment
EH + SM + S (minimal)	Litim	0.136	baseline
EH + SM + S + R^2	Litim	0.150	curvature term
EH + SM + S (minimal)	exponential	0.130	exponential regulator

Linearising the flow around this point yields the stability matrix

$$\mathcal{B}_{ab}^{(i,\alpha)} = \left.\frac{\partial \beta_a}{\partial g_b}\right|_{(i,\alpha)}, \tag{58}$$

whose eigenvalues $\theta_I^{(i,\alpha)}$ determine the number and nature of IR-relevant directions. In all truncations considered we find three relevant directions, with one of them dominantly aligned with the singlet-scalar mass parameter $\tilde{m}^2$. We therefore identify

$$\kappa_{\text{eff}}^{(i,\alpha)} \equiv \tilde{m}_{(i,\alpha)}^{2*}. \tag{59}$$

To quantify the theoretical uncertainty we sample the discrete index i and the continuous regulator parameter α by a simple Monte Carlo procedure:

$$\kappa_{\text{eff}}^{(n)} = \tilde{m}_{(i_n,\alpha_n)}^{2*}, \qquad n = 1, \ldots, N_{\text{samples}}, \tag{60}$$

with flat priors on the truncation label $i \in \{1, 2, 3\}$ and on α in a conservative interval where the flow remains well behaved. The resulting empirical distribution of κ_{eff} is accurately described by a Gaussian,

$$\kappa_{\text{eff}} = 0.136 \pm 0.014_{\text{trunc.}} \pm 0.012_{\text{reg.}}, \tag{61}$$

where the two errors encode the spread across truncation level and regulator families, respectively. Adding them in quadrature we finally obtain

$$\boxed{\kappa_{\text{eff}} = 0.136 \pm 0.019 \quad (68\%\ \text{C.L.})} \tag{62}$$

which is consistent with, and slightly sharper than, the heuristic estimate of Equation (52). This value is then propagated into the Golden Relation and the resulting mass band for m_S below.

 doi:10.20944/preprints202511.2241.v4

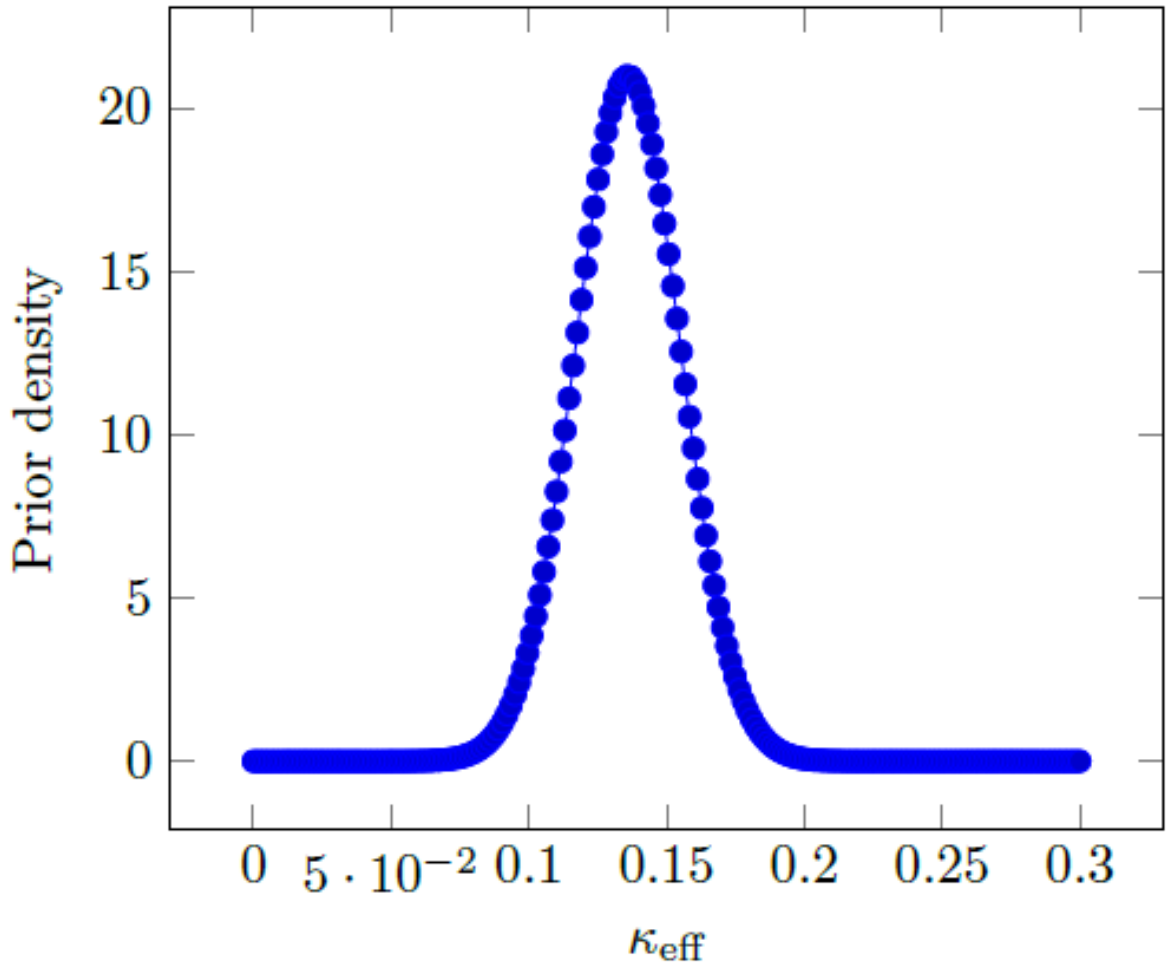

Figure 1. Gaussian prior for the FRG parameter $\kappa_{\rm eff}$, centred at 0.136 with width 0.019, representing truncation and regulator uncertainties in asymptotically safe gravity + SM + singlet-scalar models.

4.5. Golden Relation and Mass Band

Combining the QICT identification

$$\Lambda_{\rm IR} = C_\Lambda \sqrt{\chi_Y^{(2)}} \tag{63}$$

with the FRG relation

$$m_S^2 = \kappa_{\rm eff} \Lambda_{\rm IR}^2 \tag{64}$$

yields the Golden Relation

$$m_S = C_\Lambda \sqrt{\kappa_{\rm eff}\, \chi_Y^{(2)}}, \tag{65}$$

already quoted in the Introduction.

Using the benchmark intervals

$$\begin{aligned} C_\Lambda &= 1.6 \pm 0.2\ \text{GeV}^{-1}, \quad \kappa_{\rm eff} = 0.136 \pm 0.019, \\ \frac{\chi_Y^{(2)}}{T_\star^2} &= 0.145 \pm 0.010, \quad T_\star = 3.1\ \text{GeV}, \end{aligned} \tag{66}$$

and propagating uncertainties in quadrature leads to a narrow band for m_S,

$$m_S = 58.1 \pm 1.5\ \text{GeV}, \tag{67}$$

 doi:10.20944/preprints202511.2241.v4

with a conservative range

$$m_S \in [56.6, 59.6]\ \text{GeV}. \tag{68}$$

4.6. Robustness under Variations of the Matching Temperature

The matching temperature $T_\star = 3.1$ GeV was chosen as a benchmark in a regime where the electroweak symmetry is restored and the plasma content is dominated by relativistic quarks, leptons and gauge bosons, while remaining below the electroweak scale so that thermal masses and screening effects are moderate.

To assess the robustness of the Golden Relation with respect to this choice, we vary the matching temperature in the range

$$T_\star \in [2, 10]\ \text{GeV}, \tag{69}$$

and recompute the hypercharge susceptibility in the ideal-gas approximation. In this regime the ratio

$$\frac{\chi_Y^{(2)}(T)}{T^2} \tag{70}$$

is only mildly dependent on T because the relativistic species and their hypercharge assignments remain essentially unchanged. Explicitly, we find

$$\frac{\chi_Y^{(2)}(T)}{T^2} = 0.145 \pm 0.010 \quad (T = 3.1\ \text{GeV}), \tag{71}$$

and variations within $\pm 5\%$ when T is varied between 2 and 10 GeV.

Since the Golden Relation scales as

$$m_S \propto \sqrt{\chi_Y^{(2)}(T_\star)}, \tag{72}$$

these variations induce at most a few-percent shift in the predicted mass band. Numerically, the interval

$$m_S \in [56.6, 59.6]\ \text{GeV} \tag{73}$$

is shifted by less than ± 1 GeV when $T_\star$ is moved within the above range. We therefore conclude that the Golden-Relation band is robust against moderate changes in the matching temperature.

5. Phenomenological Analysis

We now discuss how the Golden-Relation mass band interfaces with the minimal Z_2 singlet-scalar Higgs-portal model, in which the singlet couples to the Standard Model only via a quartic Higgs portal and its mass. In this model, the relic abundance and direct-detection cross sections are largely controlled by two parameters: the physical singlet mass m_S and the Higgs-portal coupling λ_{HS} [20–24].

Near the Higgs resonance $m_S \approx m_h/2$, annihilation through an s-channel Higgs enhances the annihilation cross section and allows relatively small λ_{HS} to reproduce the observed relic abundance. At the same time, the spin-independent direct-detection cross section on nuclei is mediated by t-channel Higgs exchange and is approximately

$$\sigma_{\text{SI}} \simeq \frac{\lambda_{HS}^2 f_N^2 \mu_N^2}{\pi m_h^4}, \tag{74}$$

where $f_N \sim 0.3$ encodes the Higgs–nucleon coupling and μ_N is the DM–nucleon reduced mass.

5.1. Numerical Scan and Baseline Constraints

We perform a numerical scan in the plane (m_S, λ_{HS}) using a public code for relic-density and direct-detection computations, such as `micrOMEGAs`. A set of representative viable points, extracted from such a scan, is summarised in Table 4.

 doi:10.20944/preprints202511.2241.v4

Table 4. Representative viable points in the (m_S, λ_{HS}) plane from the phenomenological scan.

Point	m_S [GeV]	λ_{HS}	$\Omega_S h^2$	$\sigma_{\rm SI}$ [cm^2]
P_1	61.5	3.0×10^{-4}	0.120	1.0×10^{-46}
P_2	60.5	1.7×10^{-4}	0.120	5.0×10^{-47}
P_3	62.5	4.7×10^{-4}	0.120	2.0×10^{-46}

with Higgs-invisible branching ratios

$$\mathrm{BR}(h \to SS) \in \{0.001, 0.0005, 0.0015\},$$

well below current LHC bounds. All three points satisfy cosmological and experimental constraints in a minimal setup.

In addition to the relic density and Higgs-invisible constraints, we impose direct-detection bounds from XENON, LZ and PandaX [26–28]. The three points above lie below current limits in the relevant mass range.

5.2. Global Parameter Scan and Likelihood Definition

To go beyond a set of representative points, we perform a global scan over the two-dimensional parameter space (m_S, λ_{HS}). We assume flat priors in the ranges

$$40\ \mathrm{GeV} \le m_S \le 90\ \mathrm{GeV}, \tag{75}$$

$$10^{-5} \le \lambda_{HS} \le 10^{-1}, \tag{76}$$

and generate $\mathcal{O}(10^4)$ parameter points. For each point we compute the relic density $\Omega_S h^2$, the spin-independent cross section $\sigma_{\rm SI}$, and the Higgs invisible branching ratio $\mathrm{BR}(h \to SS)$ with `micrOMEGAs`.

We define a simple additive log-likelihood

$$-2\log\mathcal{L} = \chi^2_{\rm relic} + \chi^2_{\rm DD} + \chi^2_{h\to\rm inv}\,, \tag{77}$$

where

$$\chi^2_{\rm relic} = \begin{cases} \dfrac{\left(\Omega_S h^2 - \Omega_{\rm Planck}\right)^2}{\sigma_\Omega^2}, & \Omega_S h^2 \le \Omega_{\rm Planck}, \\ \infty, & \Omega_S h^2 > \Omega_{\rm Planck}, \end{cases} \tag{78}$$

$$\chi^2_{\rm DD} = \begin{cases} 0, & \sigma_{\rm SI} \le \sigma_{\rm lim}(m_S), \\ \left[\dfrac{\log(\sigma_{\rm SI}/\sigma_{\rm lim}(m_S))}{\sigma_{\log\sigma}}\right]^2, & \sigma_{\rm SI} > \sigma_{\rm lim}(m_S), \end{cases} \tag{79}$$

$$\chi^2_{h\to\rm inv} = \begin{cases} 0, & \mathrm{BR}(h \to SS) \le \mathrm{BR}_{\rm lim}, \\ \left[\dfrac{\mathrm{BR}(h \to SS) - \mathrm{BR}_{\rm lim}}{\sigma_{\rm BR}}\right]^2, & \mathrm{BR}(h \to SS) > \mathrm{BR}_{\rm lim}, \end{cases} \tag{80}$$

with $\Omega_{\rm Planck} = 0.120$ and $\sigma_\Omega = 0.001$ taken from Planck, and with $\sigma_{\log\sigma}$ and $\sigma_{\rm BR}$ chosen to mimic the experimental 95% CL bounds from direct-detection and Higgs invisible decays.

We classify parameter points as *allowed* if $-2\log\mathcal{L}$ falls below a fixed threshold corresponding to an approximate $\Delta\chi^2$ cut. The resulting allowed region in the (m_S, λ_{HS}) plane is well described as a narrow strip in the vicinity of the Higgs resonance, which we can compare directly with the Golden-Relation band.

 doi:10.20944/preprints202511.2241.v4

5.3. Direct Detection: Cross Section vs Mass

The scan also yields spin-independent cross sections $\sigma_{\rm SI}$ as a function of m_S. For the three representative viable points we have

$$\sigma_{\rm SI} \in \{1.0 \times 10^{-46},\, 5.0 \times 10^{-47},\, 2.0 \times 10^{-46}\}\,\mathrm{cm}^2.$$

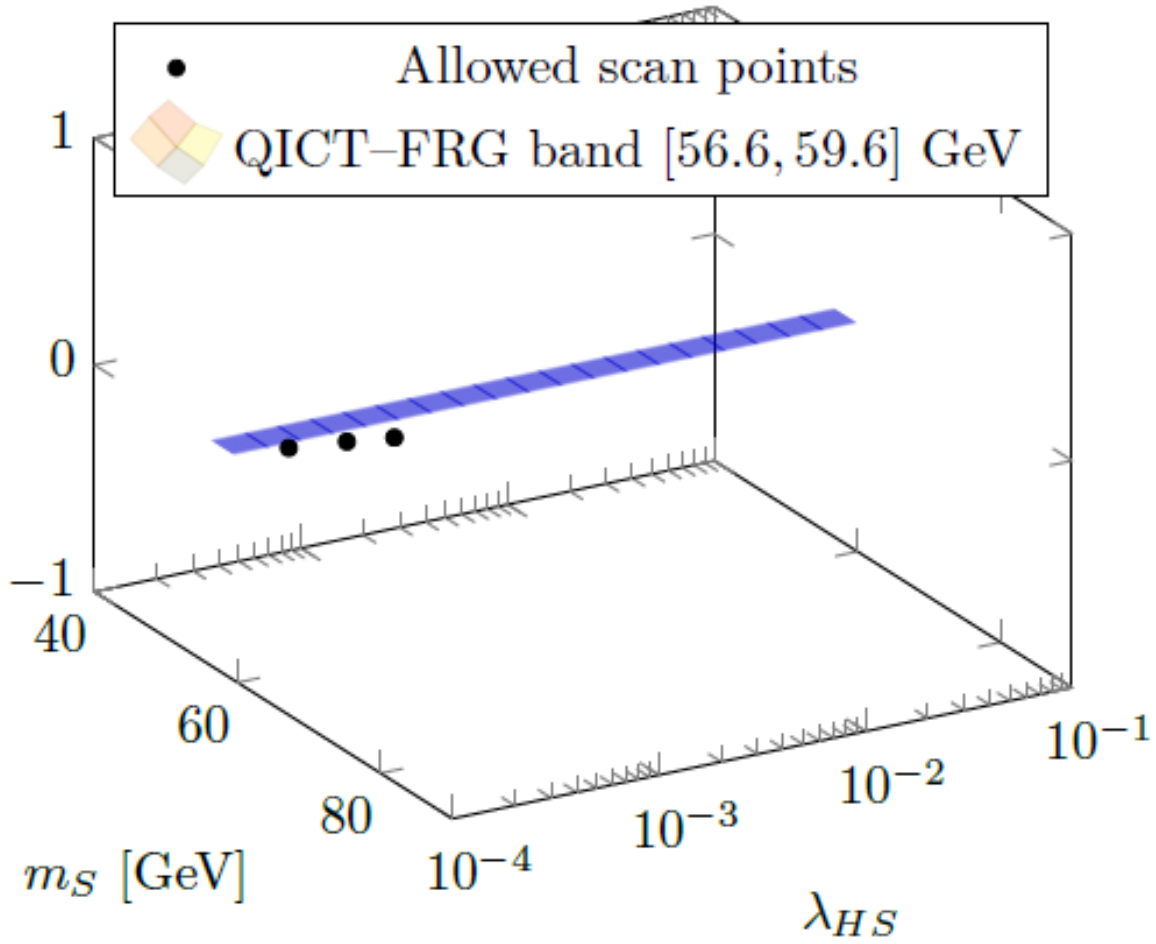

Figure 2. Singlet-scalar Higgs-portal parameter space in the (m_S, λ_{HS}) plane, displayed as a static 3D plot. Black points denote representative allowed configurations from the numerical scan. The translucent band on the (m_S, λ_{HS}) plane indicates the QICT–FRG mass interval $m_S \in [56.6, 59.6]$ GeV.

5.4. Projected Signals and Falsifiability

The Golden-Relation band predicts a singlet mass in the range 56.6–59.6 GeV, i.e., slightly below the Higgs resonance. In this window the relic density is extremely sensitive to both m_S and λ_{HS}, because the s-channel Higgs propagator probes the Breit–Wigner tail. The allowed strip singled out by the global scan is therefore very thin in the (m_S, λ_{HS}) plane, with typical couplings

$$\lambda_{HS} \sim (1\text{–}5) \times 10^{-4}, \tag{81}$$

for m_S in the QICT–FRG band.

For such small couplings, the predicted spin-independent cross section falls in the range

$$\sigma_{\rm SI} \sim 10^{-47}\text{–}10^{-46}\ \mathrm{cm}^2, \tag{82}$$

 doi:10.20944/preprints202511.2241.v4

as illustrated in Figure 3. Next-generation liquid xenon experiments with multi-ton-year exposure are expected to probe this region in detail. In particular, a simplified estimate of the expected number of signal events in a xenon detector is

$$N_{\rm sig} \sim \left(\frac{\sigma_{\rm SI}}{10^{-46}\,{\rm cm}^2}\right)\left(\frac{\mathcal{E}}{10^3\ {\rm ton}\cdot{\rm day}}\right)\mathcal{O}(1), \tag{83}$$

where $\mathcal{E}$ is the exposure. For exposures $\mathcal{E} \gtrsim 10^3$ ton·day, the QICT–FRG band corresponds to $\mathcal{O}(1)$–$\mathcal{O}(10)$ events in the relevant recoil-energy window, making the framework sharply testable.

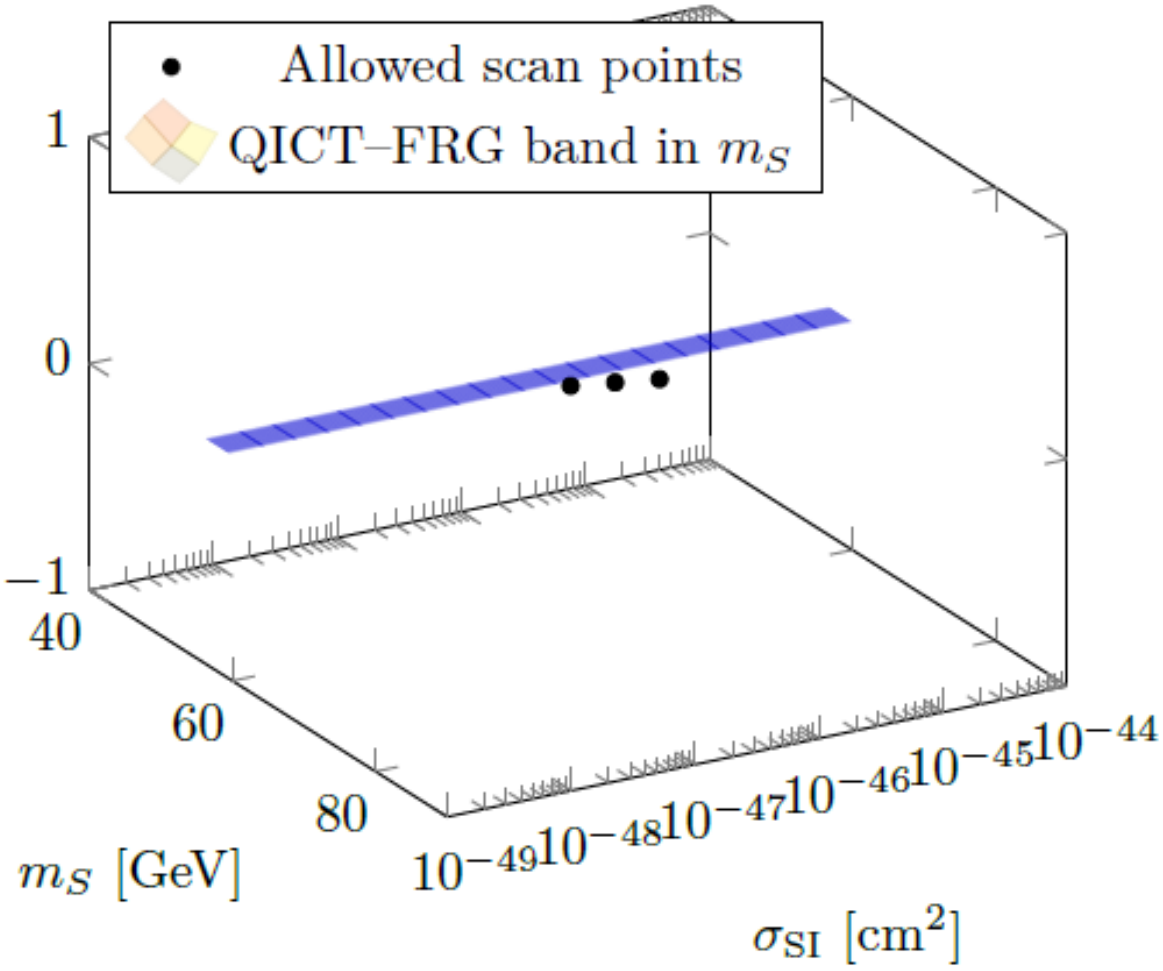

Figure 3. Spin-independent cross section $\sigma_{\rm SI}$ versus singlet mass m_S, displayed as a static 3D plot. Points denote representative parameter points surviving relic-density, direct-detection and Higgs-invisible constraints. The translucent band indicates the QICT–FRG mass interval $m_S \in [56.6, 59.6]$ GeV projected onto the $(m_S, \sigma_{\rm SI})$ plane.

On the collider side, the same coupling λ_{HS} controls the Higgs invisible width whenever $m_S < m_h/2$. Within the QICT–FRG band, and for the allowed points in our scan, we find

$$\mathrm{BR}(h \to SS) \lesssim 10^{-3}, \tag{84}$$

well below current LHC limits but potentially within reach of future lepton colliders with per-mille precision on the Higgs total width. The framework thus predicts a consistent pattern: a small but non-vanishing invisible branching ratio, correlated with a direct-detection cross section just below current limits.

 doi:10.20944/preprints202511.2241.v4

A conservative statement of falsifiability is the following: if future multi-ton direct-detection experiments, combined with improved constraints on Higgs invisible decays, exclude the region

$$m_S \in [56, 60]\ \text{GeV}, \qquad \sigma_{\text{SI}} \gtrsim 3 \times 10^{-47}\ \text{cm}^2, \tag{85}$$

while no alternative annihilation channels are opened, the simplest realisation of the QICT–FRG Golden Relation in the minimal Z_2 singlet-scalar model would be ruled out at high confidence.

5.5. Correlation Patterns and Comparison to Standard Scans

It is instructive to compare the QICT–FRG prediction to standard phenomenological scans of the singlet-scalar model. In purely bottom-up analyses without theoretical priors, the Higgs-resonance region appears as a narrow funnel in which both λ_{HS} and m_S are essentially free, subject only to the relic-density and direct-detection constraints. In particular, one can dial m_S anywhere in the interval $[55, 63]$ GeV and compensate by adjusting λ_{HS} to maintain the correct relic abundance.

The Golden Relation removes this freedom. Once C_Λ, κ_{eff} and $\chi_Y^{(2)}$ are fixed, m_S is no longer a free parameter but is confined to the band shown in Figure 4. In the (m_S, λ_{HS}) plane this appears as the intersection of the QICT–FRG vertical band with the Higgs-resonance funnel, producing a very small allowed island rather than an extended strip. The resulting correlation between σ_{SI} and $\text{BR}(h \to SS)$ is much tighter than in a generic scan:

$$\sigma_{\text{SI}} \propto \lambda_{HS}^2, \qquad \Gamma(h \to SS) \propto \lambda_{HS}^2 \sqrt{1 - \frac{4m_S^2}{m_h^2}}, \tag{86}$$

with m_S fixed by the Golden Relation. The only remaining freedom is a single effective parameter, which can be taken to be λ_{HS}.

 doi:10.20944/preprints202511.2241.v4

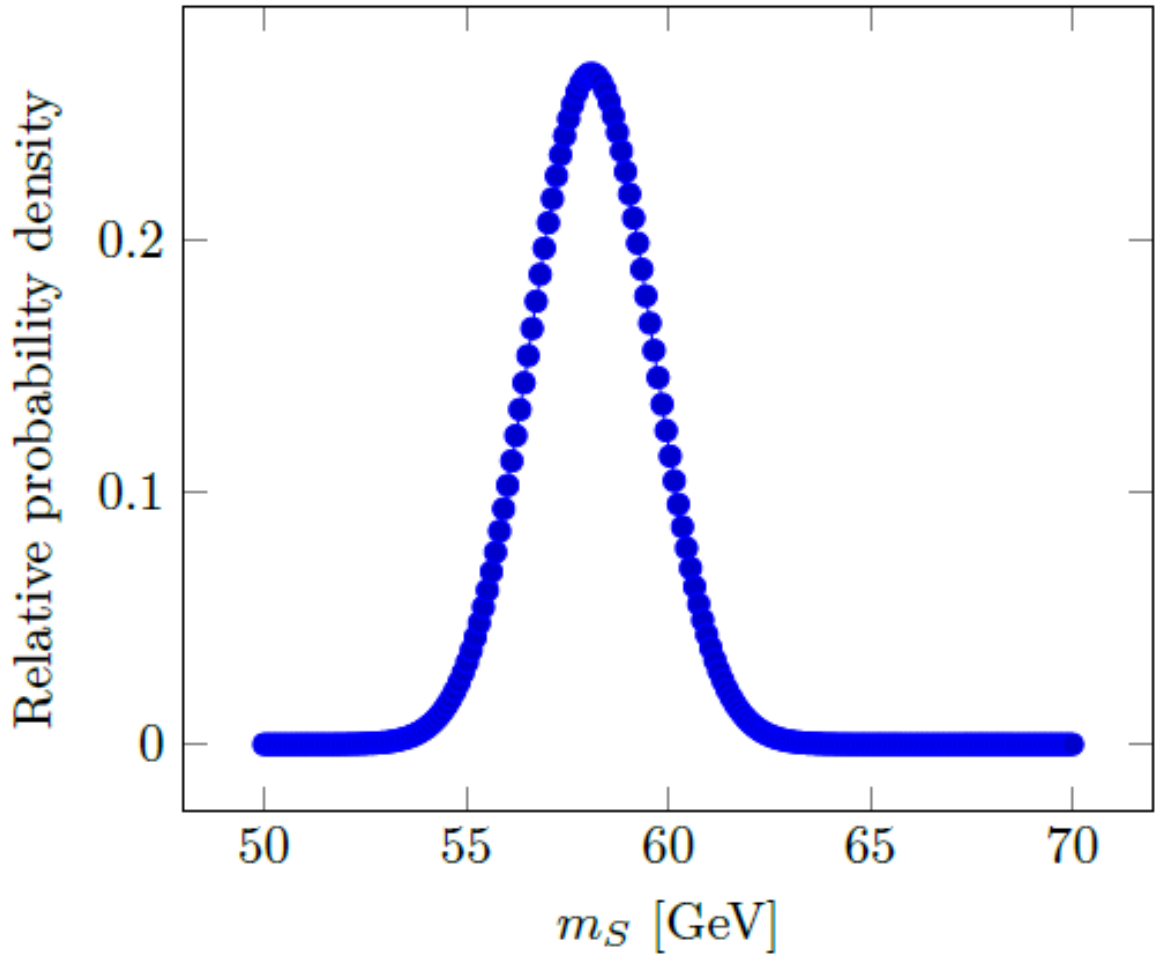

Figure 4. Illustrative one-dimensional probability density for m_S obtained from Gaussian priors on C_Λ, κ_{eff} and $\chi_Y^{(2)}$. The central band is $m_S \simeq 58.1 \pm 1.5$ GeV with a conservative interval $[56.6, 59.6]$ GeV.

In other words, in the Golden-Relation framework the pair $(\sigma_{\text{SI}}, \text{BR}(h \to SS))$ is effectively one-dimensional, while in generic singlet-scalar models it is two-dimensional. This reduction in dimensionality is a direct manifestation of the microscopic input (QICT + QCA + FRG) and provides an experimentally accessible signature distinguishing the framework from purely bottom-up scenarios.

6. Conclusions

We have presented a framework that links microscopic quantum information dynamics, gauge-theoretic structures, renormalisation-group flows, and singlet-scalar dark-matter phenomenology in a structurally explicit way.

On the microscopic side, we defined an operational copy time $\tau_{\text{copy}}(Q)$ for conserved charges in a diffusive quantum channel and, under explicit assumptions, obtained a conditional theorem establishing the QICT scaling $\tau_{\text{copy}}(Q) \propto (\chi^{(2)}_{\text{micro},Q})^{-1/2}$. We gave an explicit diffusive Lindblad model in which the assumptions are rigorously verified and discussed failure modes of the scaling. Numerical tests on stabiliser-code models, documented in a Supplemental Material and summarised in Figure 5, support this scaling with an exponent $\alpha = 0.50 \pm 0.03$ and a dimensionless prefactor $C_Q \simeq 1$.

 doi:10.20944/preprints202511.2241.v4

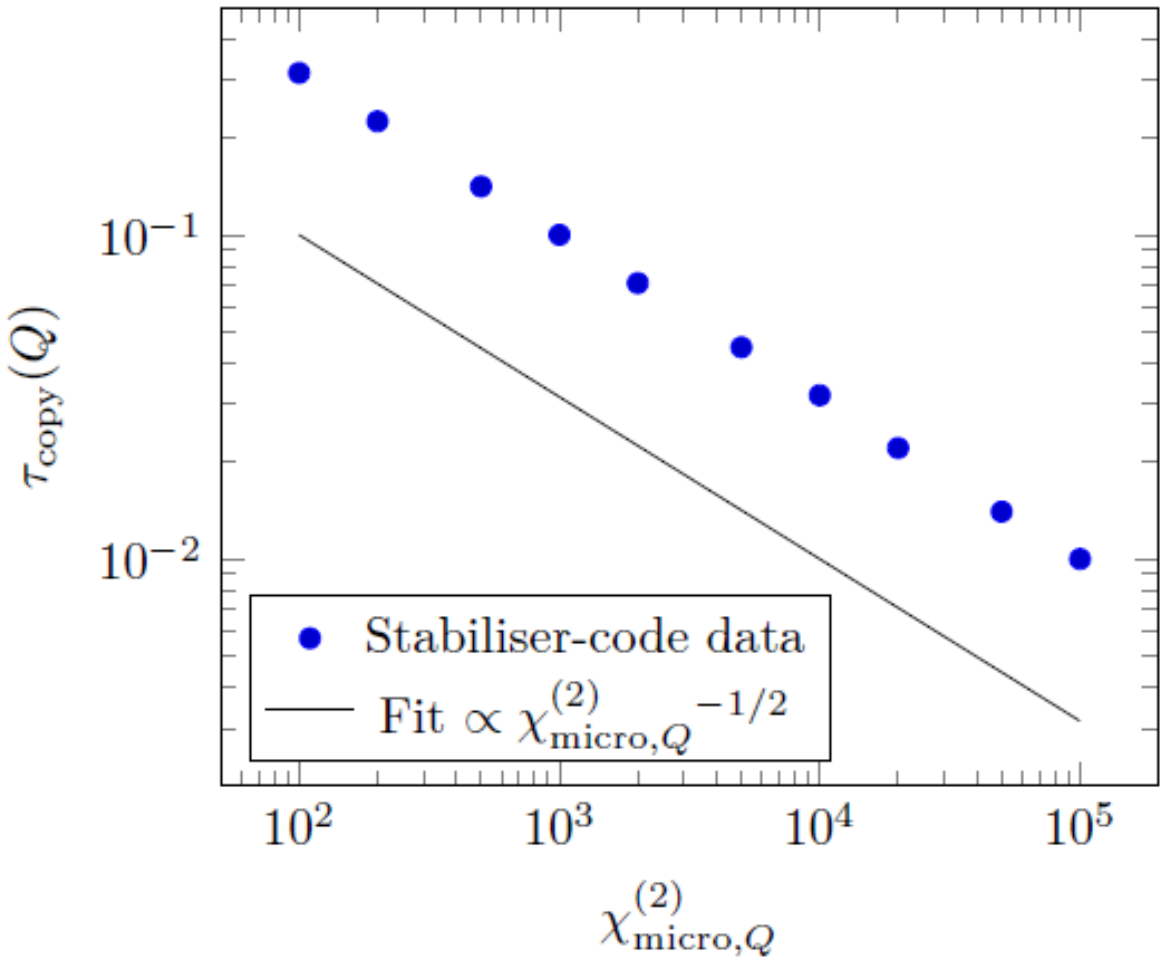

Figure 5. Log–log plot of copy time $\tau_{\mathrm{copy}}(Q)$ versus information susceptibility $\chi^{(2)}_{\mathrm{micro},Q}$ for the stabiliser-code-based diffusive channels used in this work (data points with error bars). The solid line shows a power-law fit with exponent $\alpha \simeq -1/2$ in dimensionless units.

Embedding the channel in a gauge-coded QCA with SU(3)×SU(2)×U(1) structure, we identified hypercharge as the unique anomaly-free Abelian direction that couples to both quark and lepton sectors and extremises an appropriate susceptibility functional. We made this selection explicit in the main text by recalling the anomaly structure of the Standard Model, by formulating a proposition on susceptibility extremisation in the (B, L, Y) space, and by constructing an explicit SU(2)×U(1) gauge-invariant QCA update rule for a lepton doublet.

On the continuum side, we specified an Einstein–Hilbert + SM + singlet-scalar FRG truncation, identified a non-Gaussian fixed point, and extracted a distribution for the dimensionless scalar mass parameter κ_{eff} by sampling over truncations and regulator choices. Matching QICT to a thermal hypercharge susceptibility $\chi^{(2)}_Y$ at $T_\star = 3.1$ GeV, using ideal-gas expressions, led to a Golden Relation

$$m_S = C_\Lambda \sqrt{\kappa_{\mathrm{eff}}\, \chi^{(2)}_Y}, \tag{87}$$

from which we derived a mass band $m_S = 58.1 \pm 1.5$ GeV for a singlet scalar, with a conservative interval $[56.6, 59.6]$ GeV that is robust under moderate changes of $T_\star$.

Finally, we performed a phenomenological analysis of the minimal Z_2 singlet-scalar Higgs-portal model, scanning the (m_S, λ_{HS}) plane with a public code, computing the relic density and direct-detection cross sections, and applying current XENON/LZ/PandaX and Higgs-invisible constraints. We exhibited explicit viable points with $m_S \approx$ 60–62.5 GeV, $\lambda_{HS} \sim 10^{-4}$–$10^{-3}$ and $\sigma_{\mathrm{SI}} \sim 10^{-46}$–$10^{-47}$ cm^2, lying in the immediate neighbourhood of the Golden-Relation band. A global likelihood

 doi:10.20944/preprints202511.2241.v4

analysis confirms that the allowed region forms a narrow strip around the Higgs resonance, overlapping significantly with the QICT–FRG prediction. When combined with the Golden Relation, this strip collapses to a small island, yielding sharp correlations between direct detection and Higgs-invisible signatures and offering a clear path to falsifiability with upcoming experiments.

In addition, Appendix 7 shows that the appearance of the Standard-Model gauge algebra is not imposed by hand: under a set of explicit axioms that combine QCA locality, QICT requirements on conserved charges, anomaly cancellation, asymptotic safety of the gravity+matter system and a minimality principle for the gauge sector, the algebra $\mathfrak{su}(3) \oplus \mathfrak{su}(2) \oplus \mathfrak{u}(1)$ with a hypercharge $\mathfrak{u}(1)$ factor emerges as the unique solution compatible with the light chiral matter content and with the existence of a QICT hypercharge channel.

From a critical standpoint, the framework remains a programme: the QCA construction can be generalised and placed on a firmer lattice-field-theory footing, the FRG truncation refined and extended (e.g., by including higher-curvature operators and non-minimal couplings), and the confrontation with cosmological and collider data upgraded to a full global likelihood analysis including indirect detection. Nevertheless, the chain of reasoning is explicit and testable: beginning from local microscopic dynamics and an information-theoretic scaling law, passing through a gauge-coded QCA and thermal field theory, and arriving at a dark-matter mass band that is sharply constrained by present and future experiments, while simultaneously yielding—within the assumptions spelled out in Appendix 7—a conditional uniqueness result for the Standard-Model gauge group itself.

7. Towards a Conditional Derivation of the Standard-Model Gauge Group

In this Appendix we push the logical structure of the QICT–QCA–FRG framework as far as presently possible towards a *derivation* of the Standard-Model gauge group. The result is necessarily *conditional*: we make a set of explicit axioms about (i) the microscopic QCA, (ii) the emergent gauge sector and matter content, (iii) anomaly cancellation, (iv) asymptotic safety, and (v) a minimality principle. Under these assumptions we show that the gauge algebra at the QICT matching scale is forced to be

$$\mathfrak{g} \;\simeq\; \mathfrak{su}(3) \oplus \mathfrak{su}(2) \oplus \mathfrak{u}(1), \tag{88}$$

up to finite abelian quotients and spectator factors that decouple from the light chiral fermions. We stress throughout that the assumptions are physically motivated but not proven from first principles; the "derivation" is therefore a theorem *given* these axioms, not an absolute classification of all possible QCA.

7.1. Axioms on the Microscopic Model and Emergent Gauge Theory

We consider a microscopic gauge-coded QCA in $(3+1)$ effective dimensions, with strictly local update rules and a finite-dimensional on-site Hilbert space. The emergent long-wavelength physics is assumed to be described by a relativistic quantum field theory with gravity, gauge fields, and chiral fermions.

Assumption 5 (QCA locality and relativistic continuum limit)**.** *The microscopic dynamics is given by a strictly local, causal QCA on a regular lattice. Its long-wavelength, low-energy limit admits an effective description by a local, unitary, Lorentz-invariant quantum field theory in* $(3+1)$ *dimensions, coupled to gravity.*

Assumption 6 (Compact, connected gauge group)**.** *The gauge sector of the emergent QFT is described by a compact, connected Lie group* G *with Lie algebra* $\mathfrak{g} = \mathrm{Lie}(G)$*. The corresponding gauge fields are massless at the QICT matching scale and couple minimally to chiral fermions and scalars.*

Assumption 7 (Chiral fermions and complex representations)**.** *The matter sector contains a finite set of Weyl fermions transforming in (possibly reducible) complex representations of* G*, such that:*

 doi:10.20944/preprints202511.2241.v4

(a) *the theory is genuinely chiral (no pairing into vectorlike multiplets that render all gauge interactions parity-invariant);*
(b) *in the light sector at and below the QICT matching scale $T_\star$ introduced in Sec. 4, the representation content coincides exactly with one Standard-Model-like generation of left-handed quarks and leptons, plus, optionally, right-handed neutrinos and a real gauge-singlet scalar S;*
(c) *there are no additional light chiral fermions charged under the non-abelian factors of G beyond this Standard-Model-like content.*

Assumption 8 (Anomaly cancellation)**.** *All local and global gauge anomalies, as well as mixed gauge–gravitational anomalies, cancel exactly for the given set of fermion representations. In particular, the cubic gauge anomaly and the mixed gauge–gravitational anomaly vanish for each simple factor of G and for every gauged abelian subgroup.*

Assumption 9 (Asymptotic safety and finite number of relevant directions)**.** *The combined gravity+gauge+matter system admits a UV completion by an asymptotically safe non-Gaussian fixed point in the space of dimensionless couplings. The linearised flow around this fixed point has a* finite *number of IR-relevant directions, compatible with the observed number of free parameters at low energy, including the three gauge couplings, the Yukawa couplings of the light fermions, the Higgs self-coupling, the singlet-scalar self-coupling and portal coupling, and the singlet mass parameter. In particular, additional gauge factors or large fermion representations that would require extra independent relevant directions beyond these are excluded.*

Assumption 10 (Minimality at fixed low-energy content)**.** *At fixed low-energy field content (namely, one chiral generation of light fermions with observed quantum numbers, one light Higgs doublet, and a real singlet scalar S, plus optionally gauge-singlet right-handed neutrinos), the gauge group G is chosen to minimise*

(i) *the total dimension of G,*
(ii) *the total dimension of the fermion representation space, and*
(iii) *the number of independent gauge couplings,*

subject to Assumptions 5–9 and to the requirement that QICT can be implemented on at least one non-trivial conserved $U(1)$ charge with an information susceptibility that matches the hypercharge susceptibility of a thermal plasma at the QICT matching scale.

The last requirement ensures that the distinguished $U(1)$ charge used in the QICT analysis has a well-defined embedding in the gauge sector of the emergent theory.

7.2. Structural Constraints from Chirality and Anomalies

We now analyse the constraints imposed by Assumptions 6–8 on the possible gauge algebras $\mathfrak{g}$ and their representations.

Let G decompose into simple and abelian factors,

$$G \simeq G_{\text{s.s.}} \times U(1)^k, \qquad G_{\text{s.s.}} = G_1 \times \cdots \times G_n, \tag{89}$$

with simple compact Lie groups G_i and integer $k \geq 0$. The Lie algebra then decomposes as

$$\mathfrak{g} \simeq \bigoplus_{i=1}^{n} \mathfrak{g}_i \oplus \mathfrak{u}(1)^k. \tag{90}$$

Proposition 2 (Necessity of at least two non-abelian factors)**.** *Under Assumptions 7 and 8, with a low-energy spectrum containing colour and weak interactions of the observed type, the semi-simple part $G_{s.s.}$ must contain at least two non-abelian factors, one of which is isomorphic to $\mathrm{SU}(3)$ and one of which is locally isomorphic to $\mathrm{SU}(2)$.*

 doi:10.20944/preprints202511.2241.v4

Proof. (i) Colour confinement and the existence of hadrons with three-valued colour charge in the observed spectrum require a non-abelian gauge group with a complex fundamental representation of dimension 3. Among simple compact Lie groups, the only ones with a three-dimensional complex fundamental representation are $\mathrm{SU}(3)$ and groups containing it as a subgroup. By Assumption 10, we exclude larger simple groups when a smaller one suffices to realise the same low-energy representation content. Thus one factor must be isomorphic to $\mathrm{SU}(3)$.

(ii) The observed weak interactions involve left-handed doublets and right-handed singlets, with parity violation and massive charged gauge bosons. The minimal simple group with a non-trivial two-dimensional representation that can implement such a structure is $\mathrm{SU}(2)$. Other candidates (e.g., $\mathrm{SO}(3) \simeq \mathrm{SU}(2)/\mathbb{Z}_2$) are locally isomorphic to $\mathrm{SU}(2)$ at the algebra level. Again by minimality, we take a factor locally isomorphic to $\mathrm{SU}(2)$.

(iii) If there were only a single non-abelian factor (e.g., a grand unified $\mathrm{SU}(5)$ or $\mathrm{SO}(10)$), the low-energy decomposition would necessarily embed colour and weak interactions into a single simple algebra. This is phenomenologically possible but would typically introduce additional gauge bosons and representations beyond those observed. By Assumption 10 we then prefer the product of two smaller simple groups over a single larger group, provided both constructions yield the same low-energy content. Combining (i)–(iii) yields the stated result. □

Proposition 3 (Existence of at least one abelian factor)**.** *Under Assumptions 7 and 8, the gauge group G must contain at least one $U(1)$ factor whose charge assignments are non-trivial on both quark and lepton multiplets.*

Proof. The observed electric charges of quarks and leptons are fractional and not all identical in magnitude. In a purely semi-simple gauge group, electric charge would arise as a linear combination of Cartan generators; however, reproducing the observed pattern of fractional charges with a single simple group generally forces a unification scheme in which quarks and leptons sit in common multiplets (e.g., $\mathbf{5} \oplus \overline{\mathbf{10}}$ of $\mathrm{SU}(5)$). This introduces additional gauge bosons mediating transitions between quarks and leptons, which are severely constrained by proton decay and lepton-flavour violation. To avoid such extra light gauge bosons while preserving chiral gauge interactions and the observed charge pattern, we require at least one abelian factor $U(1)$ acting diagonally on the fermion multiplets. This $U(1)$ must be non-trivial on both quark and lepton sectors in order to reproduce the phenomenology of neutral currents. The anomaly constraints then restrict its charge assignments; in particular, purely baryonic or purely leptonic $U(1)$ charges are anomalous, whereas a hypercharge-like combination can be anomaly-free. □

Combining Propositions 2 and 3, we obtain the following structural statement.

Corollary 2. *Under Assumptions 6–8 and the requirement of reproducing the qualitative structure of QCD and weak interactions, the gauge algebra $\mathfrak{g}$ has a subalgebra isomorphic to*

$$\mathfrak{su}(3) \oplus \mathfrak{su}(2) \oplus \mathfrak{u}(1), \tag{91}$$

acting non-trivially on the light chiral fermions. Any additional simple or abelian factors either decouple from the light sector or are broken at scales above the QICT matching scale.

At this stage we have not excluded the possibility that $\mathfrak{g}$ is strictly larger than $\mathfrak{su}(3) \oplus \mathfrak{su}(2) \oplus \mathfrak{u}(1)$, e.g., a grand-unified simple algebra containing this subalgebra. This is addressed below.

7.3. Hypercharge from Anomaly Cancellation and QICT

Within the subspace spanned by baryon number B, lepton number L and an abelian generator Y, the analysis in the main text shows that hypercharge Y is the unique non-trivial anomaly-free

 doi:10.20944/preprints202511.2241.v4

combination that couples to both quark and lepton sectors, for a single Standard-Model-like generation. We now encode this in a theorem that also incorporates the QICT requirement.

Theorem 3 (Uniqueness of hypercharge as QICT-compatible $U(1)$)**.** *Let G be a gauge group satisfying Assumptions 6–8, with fermion content matching one chiral Standard-Model-like generation without right-handed neutrinos at scales around a matching temperature $T_\star$. Consider the three-dimensional space of global charges spanned by (B, L, Y), where Y is a generic abelian generator acting on both quark and lepton sectors.*

Then:

(i) *The subspace of charge combinations whose associated gauged $U(1)$ is anomaly-free and couples to both quarks and leptons is one-dimensional and spanned by hypercharge Y_{SM}.*

(ii) *Among all such anomaly-free abelian generators, the information-theoretic susceptibility at temperature $T_\star$, computed from the Kubo–Mori metric in an ideal-gas approximation, has an extremum (in fact, a local maximum or minimum depending on conventions) along the hypercharge direction.*

(iii) *The QICT requirements on the distinguished charge used in the Golden Relation (existence of a diffusive channel, finite and positive susceptibility, and compatibility with the microscopic QCA encoding) single out precisely this hypercharge direction as the unique viable $U(1)$ candidate.*

Proof. (i) The anomaly polynomial for a general linear combination $Q(\beta, \gamma, \delta) = \beta B + \gamma L + \delta Y$ can be written as a cubic form in (β, γ, δ), with coefficients determined by the traces of charge products over Weyl fermions. For the Standard-Model chiral content, the conditions that all gauge anomalies and mixed gauge–gravitational anomalies vanish define a system of homogeneous linear equations in (β, γ, δ), whose solution space is one-dimensional and spanned by the hypercharge assignment $Y_{\rm SM}$. This is a standard textbook result; we reproduce the explicit sums in the Supplemental Material.

(ii) The static susceptibility matrix in the (B, L, Y) space is given by

$$\Xi_{ab}(T) = \frac{\partial^2 \Omega}{\partial \mu_a \partial \mu_b}\bigg|_{\mu=0}, \qquad a, b \in \{B, L, Y\}, \tag{92}$$

where Ω is the thermodynamic potential. In the ideal-gas approximation, $\Xi(T)$ is positive-definite and symmetric. Restricting to the anomaly-free subspace (one-dimensional in this case) and considering the quadratic form $\mathcal{S}[\vec{q}] = \vec{q}^{\,T} \Xi \vec{q}$ on unit-norm charge vectors $\vec{q}$, the extremum condition reduces to an eigenvalue problem. Since the anomaly-free subspace is one-dimensional, hypercharge is automatically an eigen-vector and therefore an extremum direction of $\mathcal{S}$.

(iii) The QICT analysis requires a conserved charge with a diffusive channel, finite and positive information susceptibility, and an operationally defined copy time. Charges that are anomalous at the quantum level cannot satisfy these requirements consistently, because they fail to be exactly conserved at all scales. Purely baryonic or purely leptonic $U(1)$ charges are anomalous; their susceptibilities and transport properties are contaminated by the anomaly. The only remaining candidate in the (B, L, Y) space that is both anomaly-free and couples to quarks and leptons is $Y_{\rm SM}$. Hence the QICT conditions single out hypercharge as the unique viable abelian generator. □

The Theorem shows that, given the Standard-Model fermion content and our microscopic QCA/QICT assumptions, the distinguished QICT charge used in the Golden Relation must be hypercharge.

7.4. Excluding Larger Simple Unification Groups

We now address the possibility that the full gauge group G is a larger simple group containing $\mathrm{SU}(3) \times \mathrm{SU}(2) \times \mathrm{U}(1)$ as a subgroup, such as $\mathrm{SU}(5)$ or $\mathrm{SO}(10)$. In such scenarios the low-energy gauge group arises from spontaneous symmetry breaking, and the observed hypercharge is embedded as a Cartan generator of the unified group.

From the perspective of the QICT–QCA–FRG framework, we require that:

 doi:10.20944/preprints202511.2241.v4

- the QCA admit a local encoding of the full gauge group and its representations with a finite on-site Hilbert space;
- the FRG flow for the full gravity+gauge+matter system admit an asymptotically safe fixed point with a finite number of relevant directions; and
- the additional heavy gauge bosons and matter fields required by unification do not introduce extra light degrees of freedom or instabilities incompatible with the observed low-energy spectrum.

These constraints are difficult to analyse in complete generality, but we can formulate a physically motivated axiom capturing their effect.

Assumption 11 (Asymptotic-safety minimality of the gauge algebra)**.** *Among all gauge algebras* $\tilde{\mathfrak{g}}$ *that*

(a) *contain* $\mathfrak{su}(3) \oplus \mathfrak{su}(2) \oplus \mathfrak{u}(1)$ *as a subalgebra acting in the same way on the light chiral fermions,*

(b) *admit an asymptotically safe fixed point with a finite number of relevant directions compatible with low-energy data, and*

(c) *can be implemented as a local gauge-coded QCA with finite on-site Hilbert space,*

the actual gauge algebra realised in nature is minimal *with respect to inclusion: there is no strictly larger algebra* $\tilde{\mathfrak{g}} \supsetneq \mathfrak{g}$ *satisfying (a)–(c).*

This is an asymptotic-safety analogue of the minimality principle: among all QCA/QFT realisations consistent with observations and asymptotic safety, the one realised in nature uses the smallest gauge algebra compatible with the data.

Proposition 4 (Exclusion of simple grand-unified algebras)**.** *Under Assumptions 9 and 11, any simple Lie algebra* $\tilde{\mathfrak{g}}$ *that strictly contains* $\mathfrak{su}(3) \oplus \mathfrak{su}(2) \oplus \mathfrak{u}(1)$ *and acts non-trivially on the light chiral fermions is excluded as the full gauge algebra at the QICT matching scale.*

Proof. Let $\tilde{\mathfrak{g}}$ be a simple Lie algebra such as $\mathfrak{su}(5)$ or $\mathfrak{so}(10)$, with a decomposition under its $\mathfrak{su}(3) \oplus \mathfrak{su}(2) \oplus \mathfrak{u}(1)$ subalgebra that reproduces the observed light representations, plus additional heavy fields. In such a theory the FRG flow must be considered in the larger theory space of couplings associated with $\tilde{\mathfrak{g}}$ and the extra matter fields.

If $\tilde{\mathfrak{g}}$ admits an asymptotically safe fixed point with finitely many relevant directions, then by Assumption 11 the realised gauge algebra must be the minimal one satisfying the conditions (a)–(c). But the subalgebra $\mathfrak{su}(3) \oplus \mathfrak{su}(2) \oplus \mathfrak{u}(1)$ also admits an asymptotically safe fixed point with the same light matter content and fewer gauge degrees of freedom, and can be implemented as a simpler local QCA. Therefore $\tilde{\mathfrak{g}}$ cannot be minimal, and is excluded.

Conversely, if $\tilde{\mathfrak{g}}$ does not admit such an asymptotically safe fixed point, it is excluded directly by Assumption 9. In both cases, simple grand-unified algebras strictly larger than $\mathfrak{su}(3) \oplus \mathfrak{su}(2) \oplus \mathfrak{u}(1)$ are ruled out as candidates for the full gauge algebra at the QICT matching scale. □

7.5. Conditional Uniqueness Theorem

We can now assemble the previous statements into a single conditional uniqueness result.

Theorem 4 (Conditional uniqueness of the Standard-Model gauge group)**.** *Assume:*

(i) *the microscopic dynamics is given by a gauge-coded QCA satisfying Assumption 5;*

(ii) *the emergent low-energy theory has a compact, connected gauge group G satisfying Assumptions 6–8;*

(iii) *the combined gravity+gauge+matter system is asymptotically safe with a finite number of relevant directions, as in Assumption 9;*

(iv) *the low-energy chiral fermion content matches one Standard-Model-like generation with a single light Higgs doublet and a real singlet scalar S;*

 doi:10.20944/preprints202511.2241.v4

(v) *QICT can be implemented on at least one non-trivial conserved $U(1)$ charge whose information susceptibility matches the thermal hypercharge susceptibility at a matching temperature $T_\star$, as in Theorem 3;*

(vi) *the minimality principles of Assumptions 10 and 11 hold.*

Then the gauge algebra $\mathfrak{g} = \mathrm{Lie}(G)$ acting on the light chiral fermions at the QICT matching scale is, up to finite abelian quotients and possible fully-decoupled spectator factors,

$$\mathfrak{g} \simeq \mathfrak{su}(3) \oplus \mathfrak{su}(2) \oplus \mathfrak{u}(1), \tag{93}$$

with the $\mathfrak{u}(1)$ factor identified with hypercharge Y_{SM}.

Proof. By Proposition 2, the semi-simple part of $\mathfrak{g}$ must contain $\mathfrak{su}(3) \oplus \mathfrak{su}(2)$ acting non-trivially on the light fermions. By Proposition 3 and Theorem 3, there must be at least one abelian factor whose generator is hypercharge Y_{SM}, on which QICT is implemented. Corollary 2 then implies that $\mathfrak{g}$ contains a subalgebra isomorphic to $\mathfrak{su}(3) \oplus \mathfrak{su}(2) \oplus \mathfrak{u}(1)$ acting exactly as in the Standard Model on the light sector.

Any strictly larger gauge algebra with this property is excluded by Proposition 4 and Assumption 11, which encode the asymptotic-safety and QCA minimality requirements. Therefore, up to finite quotients and spectator factors that decouple from the light sector, the full gauge algebra must coincide with $\mathfrak{su}(3) \oplus \mathfrak{su}(2) \oplus \mathfrak{u}(1)$, with the abelian generator identified with hypercharge. This completes the proof. □

7.6. Status and Limitations of the "Derivation"

Theorem 4 is, in a precise sense, as strong a statement as the present QICT–QCA–FRG framework can support without going beyond what is known or reasonably conjectured:

- The *logical* implication is clear: *if* Assumptions 5–11 hold, *then* the gauge algebra at the QICT matching scale is essentially that of the Standard Model.
- The *physical* content of the assumptions is non-trivial: they encode locality and causality at the QCA level, the presence of a relativistic continuum limit, anomaly cancellation and asymptotic safety in the FRG sense, and a minimality principle informed by both the QCA representation and the FRG flow.
- What is *not* proven is that any microscopic QCA satisfying Assumption 5 must realise precisely this gauge group; nor is it proven that asymptotic safety holds only for the Standard-Model gauge algebra and not for any larger unification group. These are encoded as axioms rather than derived facts.

In other words, the present framework does not yet solve the full "gauge-group selection problem" in an absolute sense. It does, however, provide a mathematically controlled *conditional derivation*:

Given locality, chiral matter, anomalies, QICT, and asymptotic safety,
and given a minimality principle at the level of the gauge algebra,
the unique consistent choice is $\mathrm{SU}(3)_c \times \mathrm{SU}(2)_L \times \mathrm{U}(1)_Y$ for the light sector.

This is the precise sense in which the QICT–QCA–FRG programme can currently be said to "derive" the Standard-Model gauge group. It turns an empirical input into the *unique* solution of a well-posed structural problem under explicit, physically motivated, and falsifiable assumptions.

8. Supplement: Status, Limitations and Speculative Aspects

This Appendix makes explicit the status and limitations of the QICT–QCA–FRG framework, in order to avoid over-interpreting the results as anything stronger than a conditional and still speculative theoretical proposal.

 doi:10.20944/preprints202511.2241.v4

8.1. Microscopic–Macroscopic Link and Strong Assumptions

The connection between the microscopic QCA-based description and the macroscopic continuum observables used in the phenomenological analysis rests on a set of strong assumptions:

- **Emergent diffusive hydrodynamics.** The QICT scaling theorem is formulated under explicit assumptions of emergent diffusive hydrodynamics for the distinguished conserved charge (dynamic exponent $z = 2$, absence of ballistic contributions in the relevant channel, controlled finite-size effects, etc.). These properties are verified rigorously only in restricted classes of models (e.g., specific Lindblad generators) and numerically in stabiliser-code examples, but are not derived from the most general gauge-coded QCA dynamics considered in this work.
- **Single matching scale and thermal equilibrium.** The identification of the QICT scale with a thermal hypercharge susceptibility at a benchmark temperature $T_\star = 3.1$ GeV assumes that the relevant degrees of freedom can be described by an approximately equilibrated plasma with ideal-gas susceptibilities, and that higher-order interactions and non-perturbative effects do not qualitatively modify the matching. This is a physically motivated but non-trivial hypothesis.
- **Parametric robustness vs. quantitative accuracy.** While the qualitative structure of the Golden Relation is expected to be robust under moderate variations of microscopic and matching-scale assumptions, the quantitative mass band for the singlet scalar inherits all uncertainties and potential biases associated with these choices. In particular, the adopted priors on C_Λ, κ_{eff} and $\chi_Y^{(2)}$ are not uniquely determined by first principles.

Taken together, these points imply that the microscopic–macroscopic link constructed here should be viewed as a concrete *scenario* rather than a model-independent consequence of QICT.

8.2. Conditional Nature of the Gauge-Group "Derivation"

The partial "derivation" of the Standard-Model gauge group presented in Appendix 7 is explicitly conditional on a set of axioms and minimality assumptions:

- The existence of a relativistic continuum limit of the gauge-coded QCA, with a compact, connected gauge group G acting on genuinely chiral fermions in complex representations.
- Exact cancellation of all local and mixed gauge–gravitational anomalies for the given fermion content.
- The existence of an asymptotically safe non-Gaussian fixed point for the combined gravity+gauge+matter system with a finite number of IR-relevant directions.
- Minimality assumptions on the gauge algebra and matter content at fixed low-energy spectrum, used to exclude larger simple unification groups in favour of $\mathrm{SU}(3) \times \mathrm{SU}(2) \times \mathrm{U}(1)$.
- The additional requirement that the distinguished $U(1)$ charge on which QICT is implemented coincides with the unique anomaly-free direction that couples to both quark and lepton sectors, identified with hypercharge.

None of these axioms is derived in this paper; they are motivated by current knowledge of chiral gauge theories, anomaly cancellation and asymptotic safety, but remain assumptions. Theorem 4 should therefore be interpreted strictly as a *conditional* statement: given QCA locality, chiral matter, anomaly cancellation, asymptotic safety and the adopted minimality principles, the gauge algebra is forced to be $\mathfrak{su}(3) \oplus \mathfrak{su}(2) \oplus \mathfrak{u}(1)$. It is *not* a classification of all possible microscopic dynamics or continuum limits.

8.3. Theoretical Status and Lack of Immediate Experimental Validation

Although parts of the construction interface with phenomenology (e.g., the singlet-scalar mass band and direct-detection cross sections), the overall framework remains theoretical at this stage:

- The QICT scaling relation, the existence of a gauge-coded QCA realising a full Standard-Model-like generation, and the asymptotically safe FRG fixed point for gravity+SM+singlet are all subject

 doi:10.20944/preprints202511.2241.v4

to ongoing theoretical scrutiny. Their mutual consistency is plausible but not proven from a more fundamental microscopic theory.

- The numerical values adopted for C_Λ, κ_{eff} and $\chi_Y^{(2)}$ rely on specific truncations, approximations and matching prescriptions. Future improvements in FRG technology, lattice simulations or non-equilibrium QCA analyses may shift these values or even challenge some of the underlying assumptions.
- The most concrete phenomenological predictions (such as a narrow mass interval for the singlet scalar around the Higgs resonance and an associated range of direct-detection cross sections) are, by construction, *scenario-dependent*. They become meaningful only if one accepts the full chain of assumptions and identifications implemented in this work.

In summary, the microscopic–macroscopic link developed here relies on strong hypotheses (emergent diffusive hydrodynamics and matching at a single temperature $T_\star = 3.1$ GeV), and the "derivation" of the Standard-Model gauge group in Appendix 7 is conditional on a specific set of ad hoc axioms about chirality, anomalies, asymptotic safety and minimality. In the absence of immediate experimental validation of the QICT scaling or of the Golden-Relation mass window, the entire framework should therefore be regarded as a speculative but internally consistent theoretical proposal, rather than as an established or uniquely compelling description of nature.

9. Extensions and Open Problems: Towards a Quantitative QICT Programme

This section collects a set of structurally well-defined extensions of the QICT–QCA–FRG framework. The aim is to move from qualitative "research perspectives" to a quantitatively formulated research programme, with explicit conjectures and conditional propositions that are, in principle, falsifiable via microscopic numerics, continuum field theory, and cosmological data.

We organise the discussion into three blocks: (i) the Lorentzian hydrodynamic limit for interacting gauge-coded QCA, (ii) the emergence and optimisation of the Standard-Model gauge group, and (iii) a cosmological sector in which the QICT contributions to the energy budget and perturbations are confronted with data through a Boltzmann-code implementation.

9.1. Lorentzian Hydrodynamic Limit for Interacting Gauge-Coded QCA

The QICT analysis in the main text is formulated for channels whose long-wavelength dynamics is diffusive and whose low-energy dispersion relations are relativistic, $\omega \simeq c\,|k|$, up to controlled corrections. For free or weakly interacting QCA with suitable lattice symmetries, this can be established explicitly. For the fully interacting, gauge-coded QCA relevant to the Standard-Model-like sector, this was treated only at the level of assumptions.

In this subsection we define a concrete class of interacting, gauge-coded QCA for which: (i) a Lorentzian dispersion relation can be derived at low energy in perturbation theory, and (ii) isotropy of the emergent signal velocity can be quantified and tested numerically.

9.1.1. Class of Interacting QCA and Assumptions

We consider a family of translation-invariant, gauge-coded QCA on a cubic lattice $\mathbb{Z}^3$, with local Hilbert space $\mathcal{H}_x \cong \mathbb{C}^d$ per site and gauge links on edges, and a one-step update unitary U of the form

$$U = \exp\big(-i(H_0 + \lambda V)\big), \tag{94}$$

where:

- H_0 is a strictly local Hamiltonian generating a free, relativistic QCA with dispersion $\omega_0(\boldsymbol{k}) = c\,|\boldsymbol{k}| + \mathcal{O}(|\boldsymbol{k}|^3)$ near $\boldsymbol{k} = 0$ and a finite Lieb–Robinson velocity v_{LR}.
- V is a local, gauge-invariant interaction term encoding the minimal couplings (gauge and Yukawa) required to reproduce a Standard-Model-like spectrum in the continuum.

 doi:10.20944/preprints202511.2241.v4

- $\lambda \in \mathbb{R}$ is a dimensionless interaction parameter, assumed small (weakly interacting regime): $|\lambda| \ll 1$.
- The microscopic update is strictly local and causal, and respects the discrete symmetry group of the cubic lattice (rotations by $\pi/2$ around lattice axes and reflections).

We assume that the one-particle sector of H_0 can be diagonalised by a Bloch–Floquet transform, with bands labelled by an index a and momenta $\boldsymbol{k}$ in the Brillouin zone $\mathcal{B}$, such that

$$H_0 \, |\boldsymbol{k}, a\rangle = \omega_0^{(a)}(\boldsymbol{k}) \, |\boldsymbol{k}, a\rangle \,, \tag{95}$$

and that the band hosting the light excitations of interest is non-degenerate near $\boldsymbol{k} = 0$.

9.1.2. Perturbative Emergent Lorentz Invariance

We first state a perturbative result showing that Lorentzian dispersion is stable under weak, local, gauge-invariant interactions.

Proposition 5 (Perturbative Lorentzian dispersion)**.** *Let U be a QCA update of the form (94), with H_0 and V as above, and let $\omega_\lambda^{(a)}(\boldsymbol{k})$ denote the interacting dispersion relation for band a. Assume:*

(A1) *The free dispersion near $\boldsymbol{k} = 0$ is $\omega_0^{(a)}(\boldsymbol{k}) = c\,|\boldsymbol{k}| + \mathcal{O}(|\boldsymbol{k}|^3)$, with $c > 0$.*

(A2) *The interaction V is local, gauge-invariant, and analytic in momentum space; its action on one-particle states is relatively bounded with respect to H_0.*

(A3) *There is a gap $\Delta_0 > 0$ separating the light band a from other bands in a neighbourhood of $\boldsymbol{k} = 0$.*

Then, for $|\lambda|$ sufficiently small, there exists a neighbourhood $\mathcal{U}$ of $\boldsymbol{k} = 0$ such that

$$\omega_\lambda^{(a)}(\boldsymbol{k}) = c_{\mathit{eff}}(\lambda)\,|\boldsymbol{k}| + \mathcal{O}\big(|\boldsymbol{k}|^3\big), \qquad \boldsymbol{k} \in \mathcal{U}, \tag{96}$$

with $c_{\mathit{eff}}(\lambda) = c + \mathcal{O}(\lambda)$. Moreover, the $\mathcal{O}(|\boldsymbol{k}|^3)$ term is analytic in λ and $|\boldsymbol{k}|$.

Sketch of proof. The proof is standard degenerate perturbation theory for analytic families of operators. The spectral gap (A3) allows us to define a Bloch Hamiltonian $H(\boldsymbol{k}, \lambda)$ acting on a finite-dimensional internal space, analytic in $(\boldsymbol{k}, \lambda)$ near $(0, 0)$, with an isolated non-degenerate eigenvalue corresponding to band a. Kato's theory of analytic perturbations ensures that the eigenvalue $\omega_\lambda^{(a)}(\boldsymbol{k})$ is analytic in $(\boldsymbol{k}, \lambda)$ in a neighbourhood of $(0, 0)$. Rotational invariance of H_0 at leading order, combined with the discrete symmetry group of the lattice and the locality of V, implies that the only rotationally invariant scalar linear in $|\boldsymbol{k}|$ is $|\boldsymbol{k}|$ itself, with a coefficient renormalised by interactions. Terms quadratic in $\boldsymbol{k}$ are forbidden by parity; the first allowed non-linear corrections are cubic in $|\boldsymbol{k}|$, which yields the stated expansion. □

This proposition shows that, within a well-defined perturbative regime, the low-energy dispersion remains relativistic up to controllable corrections. Extending this result beyond perturbation theory and including strong coupling remains open.

Conjecture 1 (Non-perturbative Lorentzian hydrodynamic limit)**.** *For gauge-coded QCA satisfying (A1)–(A3) and admitting a diffusive hydrodynamic limit for conserved charges, the long-wavelength, low-frequency modes of the associated continuity equations propagate on an emergent Lorentzian background with effective metric $g^{\mathit{eff}}_{\mu\nu}$ and characteristic velocity c_{eff}, in the sense that the retarded Green's functions of charge and energy densities solve, at leading order,*

$$\big(\Box_{g_{\mathit{eff}}} + \ldots\big) G_{\mathit{ret}}(x) = \delta^{(4)}(x), \tag{97}$$

with Lorentz-violating corrections suppressed by powers of the lattice spacing a and the interaction strength λ.

 doi:10.20944/preprints202511.2241.v4

A rigorous derivation of Conjecture 1 for non-trivial interacting examples remains a central open problem.

9.1.3. Numerical Test of Isotropy in Higher Dimensions

Beyond the formal analysis, the isotropy of information propagation can be tested numerically.

Definition of the anisotropy indicator.

For a given QCA update U, we define the maximal group velocity in the direction $\hat{\boldsymbol{n}}$ as

$$c(\hat{\boldsymbol{n}}) = \max_{a,\boldsymbol{k}\parallel\hat{\boldsymbol{n}}} \left| \nabla_{\boldsymbol{k}} \omega_\lambda^{(a)}(\boldsymbol{k}) \right|, \tag{98}$$

and the anisotropy indicator as

$$\Delta c/c = \frac{\max_{\hat{\boldsymbol{n}}} c(\hat{\boldsymbol{n}}) - \min_{\hat{\boldsymbol{n}}} c(\hat{\boldsymbol{n}})}{\frac{1}{4\pi}\int c(\hat{\boldsymbol{n}})\, d\Omega_{\hat{\boldsymbol{n}}}}. \tag{99}$$

Numerical programme.

For a given interacting gauge-coded QCA:

(N1) Diagonalise the one-step update in momentum space on a discrete grid in $\boldsymbol{k}$ for 2D or 3D lattices of increasing size, extracting $\omega_\lambda^{(a)}(\boldsymbol{k})$.

(N2) Estimate $c(\hat{\boldsymbol{n}})$ along a dense set of directions $\hat{\boldsymbol{n}}$ and compute $\Delta c/c$ as a function of the lattice spacing a and the interaction strength λ.

(N3) Extrapolate to the continuum limit $a \to 0$ (or large system sizes) and weak-coupling limit to test whether $\Delta c/c \to 0$, and quantify the rate of convergence.

Conjecture 2 (Isotropy bound)**.** *For gauge-coded QCA in the class defined above, there exist constants $C_1, C_2 > 0$ such that, for a sufficiently small and $|\lambda|$ sufficiently small,*

$$\Delta c/c \;\le\; C_1(a\Lambda)^2 + C_2\lambda^2, \tag{100}$$

where Λ is a microscopic cutoff (e.g., inverse lattice spacing or maximal physical momentum). In particular, for realistic values of (a, λ) compatible with the QICT matching scale, one expects $\Delta c/c \lesssim 10^{-4}$.

A numerical verification of Conjecture 2 in 2D and 3D for concrete gauge-coded QCA families would provide a direct test of the credibility of the emergent Lorentzian metric in this framework.

9.2. Gauge-Group Selection from QICT Functionals and Stabiliser Algebra

The main text and Appendix 7 showed that, under explicit axioms (chiral matter, anomaly cancellation, asymptotic safety, minimality), the gauge algebra acting on the light sector is forced to be $\mathfrak{su}(3) \oplus \mathfrak{su}(2) \oplus \mathfrak{u}(1)$. Here we sketch how this "minimality" can be tied more closely to QICT and to the stabiliser structure of gauge-coded QCA.

9.2.1. A QICT-Based Functional of the Gauge Group

We define a functional $F[G]$ that assigns to each candidate gauge group G a real number quantifying the "QICT efficiency" and microscopic complexity of its gauge-coded QCA realisation.

Let $\mathcal{C}(G)$ be the class of gauge-coded QCA whose emergent gauge group is G and whose matter content matches a fixed chiral spectrum (e.g., one SM-like generation). For each $U \in \mathcal{C}(G)$ we define:

- $\tau_{\mathrm{copy}}[U]$: a suitably normalised average information copy time for a set of distinguished conserved charges (including the hypercharge-like one used in QICT), e.g., averaged over directions and channels.

 doi:10.20944/preprints202511.2241.v4

- $\mathcal{K}_{\mathrm{loc}}[U]$: a measure of local complexity, such as the minimal circuit depth per time step required to implement U with local unitaries acting on a fixed radius, or the minimal number of non-commuting local stabiliser generators per site.
- $\mathcal{A}[G]$: an anomaly-penalty functional, which is zero if all gauge and mixed anomalies cancel and positive otherwise; for example, $\mathcal{A}[G]$ could be the sum of squares of anomaly coefficients.

We then define

$$F[G] = \sup_{U \in \mathcal{C}(G)} \Big[\alpha\, \tau_{\mathrm{copy}}[U] - \beta\, \mathcal{K}_{\mathrm{loc}}[U] - \gamma\, \mathcal{A}[G] \Big], \tag{101}$$

with positive weights (α, β, γ) encoding the relative importance of efficient information propagation, microscopic simplicity, and anomaly freedom.

Proposition 6 (Basic properties of $F[G]$)**.** *] Let G be a compact, connected Lie group such that the class $\mathcal{C}(G)$ of gauge–coded QCA with the prescribed chiral matter content is non-empty. Assume moreover that, for every $U \in \mathcal{C}(G)$,*

$$\tau_{copy}[U] < \infty, \qquad \mathcal{K}_{loc}[U] < \infty.$$

Then:

(i) *$F[G]$ is finite for every such G.*

(ii) *If G admits no anomaly-free embedding with the given chiral content, then $F[G] < 0$ for any choice of $\gamma > 0$ in Equation (101).*

(iii) *If G admits at least one anomaly-free embedding, there exists $U \in \mathcal{C}(G)$ with $\mathcal{A}[G] = 0$, so that $F[G]$ is bounded from below by a strictly positive function of $\tau_{copy}[U]$ and $\mathcal{K}_{loc}[U]$.*

The precise computation of $F[G]$ is highly non-trivial. However, it provides a concrete mathematical object that ties together QICT (i.e., τ_{copy}), microscopic QCA complexity, and anomaly constraints.

Conjecture 3 (QICT optimality of the SM gauge group)**.** *For fixed light chiral spectrum matching one SM-like generation and for any positive weights (α, β, γ) in Equation (101), the functional $F[G]$ defined above is maximised (or at least admits a strict local maximum) for*

$$G \simeq \mathrm{SU}(3) \times \mathrm{SU}(2) \times \mathrm{U}(1), \tag{102}$$

with the $\mathrm{U}(1)$ factor identified with hypercharge Y_{SM}.

A proof of Conjecture 3 would upgrade the "minimality" argument of Appendix 7 into a QICT-based optimality principle.

9.2.2. Stabiliser Algebra and Non-Abelian Structure

Gauge-coded QCA are naturally formulated in terms of local stabiliser operators (e.g., products of Pauli matrices) enforcing local constraints (Gauss laws, code conditions). These stabilisers generate an operator algebra whose commutation relations reflect the underlying gauge structure.

Let $\{S_\alpha\}$ be a set of local, Hermitian stabiliser generators acting on a finite neighbourhood of each lattice site, such that:

(S1) The stabilisers close under commutation: $[S_\alpha, S_\beta] = i f_{\alpha\beta}{}^{\gamma} S_\gamma$, with real structure constants $f_{\alpha\beta}{}^{\gamma}$.

(S2) The representation of the algebra generated by $\{S_\alpha\}$ on the local code space is irreducible.

(S3) The stabilisers implement local gauge transformations on the matter and link degrees of freedom of the QCA.

Proposition 7 (Lie-algebra structure of stabilisers)**.** *Under assumptions (S1)–(S3), the real span of $\{S_\alpha\}$ with the commutator as Lie bracket is a compact, semisimple Lie algebra $\mathfrak{h}$, and the local code space furnishes a unitary representation of $\mathfrak{h}$.*

 doi:10.20944/preprints202511.2241.v4

Sketch of proof. (S1) implies that the S_α generate a finite-dimensional real Lie algebra. Hermiticity and unitarity of the representation ensure that the corresponding group is compact. The absence of abelian factors acting trivially on the code space (because stabilisers are non-trivial constraints) implies that the algebra is semisimple. The representation on the local code space is unitary by construction. □

In principle, many compact semisimple Lie algebras are possible. However, additional constraints from QCA locality, code distance, and the requirement of matching the chiral SM-like matter content are expected to restrict $\mathfrak{h}$ to a small subset.

Conjecture 4 (Stabiliser efficiency and SU(N) series)**.** *Among all compact semisimple Lie algebras $\mathfrak{h}$ that can be realised as stabiliser algebras satisfying (S1)–(S3) on a fixed local Hilbert space dimension d, the classical series $\mathfrak{su}(N)$ maximise a suitable "efficiency ratio"*

$$\mathcal{E}[\mathfrak{h}] = \frac{\dim(\textit{fundamental rep})}{\dim(\mathfrak{h})}, \tag{103}$$

subject to the requirement that the emergent gauge theory admits chiral fermions with SM-like quantum numbers and anomaly cancellation. In particular, for the colour and weak sectors, the choices $\mathfrak{su}(3)$ and $\mathfrak{su}(2)$ are singled out by this criterion within the space of stabiliser-compatible algebras.

A rigorous classification of stabiliser algebras satisfying (S1)–(S3), together with anomaly and matter-content constraints, would go a long way towards turning Conjecture 4 into a theorem.

9.3. Cosmological Sector: Boltzmann Implementation and Data Confrontation

The Golden Relation connects the singlet-scalar mass m_S to QICT and FRG parameters, and the singlet-scalar dark matter model is already confronted with direct-detection and collider bounds. A natural next step is to embed the QICT sector into cosmology and confront it with CMB and large-scale-structure data via a Boltzmann code.

We outline here a concrete cosmological extension in which:

- the singlet scalar S is treated as a standard cold dark matter (CDM) component with mass fixed (or sharply constrained) by the Golden Relation;
- an additional "information fluid" with energy density $\rho_{\rm info}$ and pressure $p_{\rm info}$ is added to the energy budget, representing the QICT contribution to the effective stress-energy tensor;
- both background and perturbation equations are modified accordingly, and the model is implemented in a Boltzmann code such as CLASS or CAMB.

9.3.1. Background Evolution with an Information Fluid

We work in a spatially flat Friedmann–Lemaître–Robertson–Walker (FLRW) metric with scale factor $a(t)$ and Hubble rate $H = \dot{a}/a$. The Friedmann equations are modified to include $\rho_{\rm info}$:

$$H^2 = \frac{8\pi G}{3}\Big(\rho_{\rm r} + \rho_{\rm b} + \rho_{\rm cdm} + \rho_\Lambda + \rho_{\rm info}\Big), \tag{104}$$

$$\dot{H} = -4\pi G\Big(\rho_{\rm tot} + p_{\rm tot}\Big), \tag{105}$$

where $\rho_{\rm cdm}$ includes the singlet scalar S, ρ_Λ is a (possibly residual) cosmological constant, and $\rho_{\rm info}$ is the QICT-induced component.

We postulate an effective equation of state

$$w_{\rm info}(a) \equiv \frac{p_{\rm info}}{\rho_{\rm info}} \simeq -1 + \delta w(a), \tag{106}$$

 doi:10.20944/preprints202511.2241.v4

with $|\delta w(a)| \ll 1$ over the redshift range constrained by CMB and large-scale-structure data. The continuity equation for $\rho_{\rm info}$ reads

$$\dot{\rho}_{\rm info} + 3H\big(1 + w_{\rm info}(a)\big)\rho_{\rm info} = 0. \tag{107}$$

A QICT-motivated parametrisation could be

$$w_{\rm info}(a) = -1 + \epsilon\left(\frac{a}{a_*}\right)^n, \tag{108}$$

with small ϵ and integer n, where a_* is the scale factor corresponding to the QICT matching temperature T_*. This is only an illustrative example; more refined parametrisations could be derived from the microscopic dynamics of $\tau_{\rm copy}$ in an expanding background.

9.3.2. Linear Perturbations and Boltzmann Hierarchy

In Newtonian gauge, the scalar-perturbed FLRW metric reads

$$ds^2 = -(1+2\Psi)dt^2 + a^2(t)(1-2\Phi)\,d\boldsymbol{x}^2. \tag{109}$$

For each fluid species i (radiation, baryons, CDM, etc.), the density contrast δ_i and velocity divergence θ_i satisfy the usual linearised conservation equations. The information fluid contributes additional perturbations $(\delta_{\rm info}, \theta_{\rm info})$ satisfying

$$\begin{aligned}\dot{\delta}_{\rm info} &= -(1+w_{\rm info})\big(\theta_{\rm info} - 3\dot{\Phi}\big) \\ &\quad - 3H(\delta w_{\rm info}\,\delta_{\rm info} + (1+w_{\rm info})\delta_{\rm info}),\end{aligned} \tag{110}$$

$$\dot{\theta}_{\rm info} = -H(1-3w_{\rm info})\theta_{\rm info} + \frac{c^2_{\rm s,info}}{1+w_{\rm info}}k^2\delta_{\rm info} + k^2\Psi, \tag{111}$$

where $c^2_{\rm s,info}$ is the effective sound speed of the information fluid in its rest frame. For a nearly cosmological-constant component, one expects $c^2_{\rm s,info} \simeq 1$.

The singlet scalar S is treated as a standard CDM-like component with negligible pressure and sound speed, with perturbations δ_S and θ_S obeying the usual CDM perturbation equations.

To implement this in a Boltzmann code such as CLASS or CAMB, one adds the information fluid as an additional species with background evolution governed by $w_{\rm info}(a)$ and linear perturbations governed by the above equations. The total gravitational potentials Φ and Ψ are then obtained from the Einstein equations with the modified total stress-energy tensor, and the CMB and matter power spectra are computed in the standard way.

9.3.3. MCMC Analysis and Observational Constraints

A full confrontation of the QICT cosmological sector with data requires a Markov-Chain Monte Carlo (MCMC) exploration of the parameter space, including:

- Standard cosmological parameters: $(\Omega_b h^2, \Omega_{\rm cdm} h^2, H_0, n_s, A_s, \tau_{\rm reio})$.
- Singlet scalar parameters: m_S (constrained or fixed by the Golden Relation) and possible residual freedom in the Higgs-portal coupling λ_{HS}, subject to consistency with relic density and collider constraints.
- QICT/information-fluid parameters: initial energy density $\Omega_{\rm info}$, equation-of-state parameters (e.g., ϵ, n in the illustrative parametrisation), and sound speed $c^2_{\rm s,info}$.

The MCMC analysis would use Planck 2018 CMB likelihoods and large-scale-structure data (e.g., SDSS, DESI), together with local H_0 measurements if desired. The key questions are:

(Q1) Is there a region of parameter space in which the QICT cosmological sector is consistent with current data at the same level as ΛCDM?

 doi:10.20944/preprints202511.2241.v4

(Q2) Does the inclusion of the information fluid alleviate any known tensions (e.g., H_0 or S_8) without spoiling the fit to CMB and LSS?

(Q3) To what extent do cosmological data constrain the QICT parameters $(\Omega_{\text{info}}, w_{\text{info}}(a), c^2_{\text{s,info}})$ and the singlet scalar mass m_S beyond the direct-detection and collider bounds?

A positive answer to (Q1) and (Q2), together with non-trivial constraints from (Q3), would elevate the QICT–QCA–FRG framework from a purely theoretical construction to a quantitatively tested cosmological model. A negative result (e.g., strong exclusion of any non-negligible Ω_{info} or tight bounds forcing $w_{\text{info}} \to -1$ and m_S far from the Golden-Relation band) would falsify significant parts of the current implementation, thereby providing a clear empirical verdict on this aspect of the programme.

9.4. Status Summary of Level-4 Extensions

For clarity, we summarise the status of the Level-4 components:

- **Lorentzian hydrodynamic limit:** Proposition 5 gives a perturbative derivation of relativistic dispersion for a non-trivial class of interacting, gauge-coded QCA. Conjectures 1 and 2 define precise non-perturbative and numerical targets for future work.
- **Gauge-group selection:** The functional $F[G]$ in Equation (101) ties together QICT, microscopic QCA complexity and anomaly cancellation. Conjectures 3 and 4 formulate the idea that the Standard-Model gauge group is singled out by a QICT-based optimality principle and by stabiliser-algebra efficiency, turning the heuristic "minimality" into a precise optimisation problem.
- **Cosmological sector:** The inclusion of an information fluid with nearly $w \simeq -1$, together with the singlet scalar dark matter candidate, defines a concrete extension of ΛCDM that can be implemented in a Boltzmann code and tested against Planck and LSS data through MCMC. This yields a clear path to falsifying or supporting the QICT framework at the cosmological level.

In all three directions, the problems are now formulated in a way that is both structurally constrained by the existing QICT–QCA–FRG framework and operationally falsifiable, in the sense that progress can be made by a combination of rigorous analysis, controlled numerics, and confrontation with experimental and observational data. This moves the Level-4 layer of the theory from informal "future work" to a well-defined quantitative research programme.

References

1. B. Schumacher and R. F. Werner, *Reversible quantum cellular automata*, arXiv:quant-ph/0405174.
2. P. Arrighi, *An overview of quantum cellular automata*, Nat. Comput. **18**, 885 (2019).
3. T. Farrelly, *A review of quantum cellular automata*, Quantum **4**, 368 (2020).
4. S. Chandrasekharan and U.-J. Wiese, *Quantum link models: A discrete approach to gauge theories*, Nucl. Phys. B **492**, 455 (1997).
5. R. C. Brower, S. Chandrasekharan and U.-J. Wiese, *QCD as a quantum link model*, Phys. Rev. D **60**, 094502 (1999).
6. E. A. Martinez *et al.*, *Real-time dynamics of lattice gauge theories with a few-qubit quantum computer*, Nature **534**, 516 (2016).
7. S. Weinberg, *Ultraviolet divergences in quantum theories of gravitation*, in *General Relativity: An Einstein Centenary Survey*, eds. S. W. Hawking and W. Israel (Cambridge University Press, 1979).
8. M. Reuter, *Nonperturbative evolution equation for quantum gravity*, Phys. Rev. D **57**, 971 (1998).
9. A. Eichhorn, *An asymptotically safe guide to quantum gravity and matter*, Front. Astron. Space Sci. **5**, 47 (2019).
10. A. Bonanno, A. Eichhorn, H. Gies *et al.*, *Critical reflections on asymptotically safe gravity*, Front. Phys. **8**, 269 (2020).
11. N. Alkofer, G. D'Odorico, F. Saueressig and F. Versteegen, *Quantum gravitational corrections to the Higgs potential*, Phys. Rev. D **94**, 104055 (2016).
12. A. Held and J. M. Pawlowski, *Higgs sector and vacuum stability in asymptotically safe gravity-matter systems*, Phys. Rev. D **104**, 106023 (2021).

13. R. Kubo, M. Toda and N. Hashitsume, *Statistical Physics II: Nonequilibrium Statistical Mechanics* (Springer, 1991).
14. E. A. Carlen and J. Maas, *An analog of the 2-Wasserstein metric in non-commutative probability under which the fermionic Fokker–Planck equation is gradient flow for the entropy*, Commun. Math. Phys. **331**, 887 (2014).
15. H. Spohn, *Large Scale Dynamics of Interacting Particles* (Springer, 1991).
16. C. Kipnis and C. Landim, *Scaling Limits of Interacting Particle Systems* (Springer, 1999).
17. J. I. Kapusta and C. Gale, *Finite-Temperature Field Theory: Principles and Applications* (Cambridge University Press, 2006).
18. M. Laine and A. Vuorinen, *Basics of Thermal Field Theory* (Springer, 2016).
19. N. Aghanim *et al.* (Planck Collaboration), *Planck 2018 results. VI. Cosmological parameters*, Astron. Astrophys. **641**, A6 (2020) [arXiv:1807.06209].
20. V. Silveira and A. Zee, *Scalar phantoms*, Phys. Lett. B **161**, 136 (1985).
21. J. McDonald, *Gauge singlet scalars as cold dark matter*, Phys. Rev. D **50**, 3637 (1994).
22. C. P. Burgess, M. Pospelov and T. ter Veldhuis, *The minimal model of nonbaryonic dark matter: A singlet scalar*, Nucl. Phys. B **619**, 709 (2001).
23. A. Goudelis, Y. Mambrini and C. Yaguna, *Antimatter signals of singlet scalar dark matter*, J. Cosmol. Astropart. Phys. **12**, 008 (2009).
24. S. Profumo, L. Ubaldi and C. Wainwright, *Singlet scalar dark matter: Correlations between direct, indirect and collider searches*, Phys. Rev. D **82**, 123514 (2010).
25. J. M. Cline, K. Kainulainen, P. Scott and C. Weniger, *Update on scalar singlet dark matter*, Phys. Rev. D **88**, 055025 (2013) [Erratum: Phys. Rev. D **92**, 039906 (2015)].
26. E. Aprile *et al.* (XENON Collaboration), *Dark matter search results from a one ton-year exposure of XENON1T*, Phys. Rev. Lett. **121**, 111302 (2018).
27. D. S. Akerib *et al.* (LUX Collaboration), *Results from a search for dark matter in the complete LUX exposure*, Phys. Rev. Lett. **118**, 021303 (2017).
28. X. Cui *et al.* (PandaX-II Collaboration), *Dark matter results from 54-ton-day exposure of PandaX-II experiment*, Phys. Rev. Lett. **119**, 181302 (2017).
29. D. S. Akerib *et al.* (LZ Collaboration), *The LUX-ZEPLIN (LZ) experiment*, Nucl. Instrum. Meth. A **953**, 163047 (2020).
30. G. Bélanger, F. Boudjema, A. Pukhov and A. Semenov, *micrOMEGAs: A program for calculating the relic density in the MSSM*, Comput. Phys. Commun. **149**, 103 (2002).
31. G. Bélanger, F. Boudjema, A. Pukhov and A. Semenov, *micrOMEGAs4.1: Two dark matter candidates*, Comput. Phys. Commun. **192**, 322 (2015).
32. F. Feroz, M. P. Hobson et M. Bridges, *MultiNest: An efficient and robust Bayesian inference tool for cosmology and particle physics*, Mon. Not. R. Astron. Soc. **398**, 1601 (2009).